# Bi-cellular wall modifications during *Bdellovibrio bacteriovorus* predation include pore formation and L,D-transpeptidase mediated prey strengthening

Erkin Kuru[1,6∫], Carey Lambert[2∫], Jonathan Rittichier[3,6], Rob Till[2], Adrien Ducret[1,4], Adeline Derouaux[5,7], Joe Gray[5], Jacob Biboy[5], Waldemar Vollmer[5], Michael VanNieuwenhze[3], Yves V. Brun[1] and R. Elizabeth Sockett[2]*

[∫]These authors contributed equally.

*Corresponding Author; liz.sockett@nottingham.ac.uk

[1] Department of Biology, Indiana University Bloomington, Bloomington, IN 47405 USA

[2] School of Life Sciences, Nottingham University, Queen's Medical Centre, Nottingham NG7 2UH UK.

[3] Department of Chemistry, Indiana University Bloomington, Bloomington, IN 47405 USA

[4] Bases Moléculaires et Structurales des Systèmes Infectieux, IBCP, Université Lyon 1, CNRS, UMR 5086, 7 passage du Vercors, 69367 Lyon Cedex 07, France

[5] The Centre for Bacterial Cell Biology, Baddiley Clark Building, Medical School, Newcastle University, Richardson Road, Newcastle upon Tyne, NE2 4AX UK

[6] Present address: Department of Genetics, Harvard Medical School, Boston, MA 02115, USA

[7] Present address: Xpress Biologics, Tour GIGA B34 (+3), Avenue de l'Hôpital, 11, B-4000 Liège (Sart-Tilman), Belgium

Modification of essential bacterial peptidoglycan (PG) containing cell walls can lead to antibiotic resistance, for example β-lactam resistance by L,D-transpeptidase activities. Predatory *Bdellovibrio bacteriovorus* are naturally antibacterial and combat infections by traversing, modifying and finally destroying walls of Gram-negative prey bacteria, modifying their own PG as they grow inside prey. Historically, these multi-enzymatic processes on two similar PG walls have proved challenging to elucidate. Here, with a PG labelling approach utilizing timed pulses of multiple fluorescent D-amino acids (FDAAs), we illuminate dynamic changes that predator and prey walls go through during the different phases of bacteria:bacteria invasion. We show formation of a reinforced circular port-hole in the prey wall; L,D-transpeptidase$_{Bd}$ mediated D-amino acid modifications strengthening prey PG during *Bdellovibrio* invasion and a zonal mode of predator-elongation. This process is followed by unconventional, multi-point and synchronous septation of the intracellular *Bdellovibrio*, accommodating odd- and even-numbered progeny formation by non-binary division.

## Article

Peptidoglycan (PG) is a shape-determining macromolecule common to the bacterial domain. The mature PG wall of bacteria is made by glycan polymerization and peptide crosslinking of a D-amino acid-rich muramyl pentapeptide subunit (**Figure 1a**). These crosslinks give the PG wall its essential load-bearing properties against the bacterial cell's turgor pressure and are made in two basic ways; either 3-4 crosslinks catalysed by normally essential and common Penicillin Binding Proteins (PBP) or 3-3 crosslinks catalysed by normally disposable, variable, L,D-transpeptidases (Ldt) (**Figure 1b**)[1].

Although PBPs and Ldts are evolutionarily and structurally distinct transpeptidases, research in diverse bacteria showed that both enzyme types can exchange a range of naturally occurring D-amino acids (DAAs) with the 5$^{th}$ and 4$^{th}$ position D-alanines in the peptide stems of PG subunits, respectively[2-4] (**Figure 1b**). Such exchanges are associated with changes in

a variety of biophysical properties of the wall[5,6], in particular the strength (as determined by osmolarity challenge[2,7]) in some bacteria. Substrate promiscuity of these transpeptidases toward a diverse set of DAAs[8] has allowed the development of fluorescent D-amino acids (FDAAs) and their implementation as a means to visualize PG dynamics *in situ*[9-12]

*Bdellovibrio bacteriovorus* (approximately 1.0 x 0.3 µm) prey upon (larger) Gram-negative bacterial species by breaching the prey outer-membrane, residing in the modified prey periplasm (forming the "bdelloplast"), resealing and growing within[13,14], before finally bursting out to invade more prey (**Figure 1c)**. The prey are killed some 20 minutes into predation when electron transport ceases as predator molecules pass across the prey inner membrane[15], however the prey bdelloplast is kept intact for 4 hours to allow "private dining" and consumption of prey contents by the predator. Early electron microscopic work[16,17] led to the assumptions that the invading *B. bacteriovorus* would squeeze through the outer layers of the prey bacterium, degrading some type of entry pore in the prey PG containing cell wall, re-sealing this, and modifying the rest of the prey PG. However, as the biochemically similar walls were obscured at the points of contact between the two bacterial cells, this bi-cellular multi-enzymatic process has, until now, been difficult to analyse. Therefore, other than recent work showing the mechanisms of prey cell rounding[18], self-protection from auto-rounding[19] and marking of the wall for later destruction[20] *B. bacteriovorus* wall-invasion dynamics and enzymology has remained a subject of conjecture.

Here, we combine three differently coloured FDAAs[9] in a timed series (**Figure 1d-e)** to illuminate dynamic PG modifications during bacterial predation, simultaneously, in two bacterial species. 3D- Structured Illumination Microscopy (3D-SIM), resolved the *B. bacteriovorus* processes of :- i) breaching the prey PG, ii) constructing a reinforced port-hole in the prey cell wall, iii) resealing the port-hole after entry, iv) modifying the prey PG with L,D-transpeptidases, and v) eventually achieving filamentous, intra-bacterial zonal cell growth and synchronous, multi-site septation.

## Results

### Multi-colour FDAA microscopy reveals prey versus predator cell wall modifications during invasion

A synchronous predatory invasion co-culture of *E. coli* prey cells pre labelled with a red FDAA, TADA, and *B. bacteriovorus* predator cells pre-labelled with a green FDAA, BADA, was established, and this invasive culture was further pulse-labelled with a blue FDAA, HADA, for 10 min at key points during the predation process. The cells were then fixed, washed, and imaged (**Figure 1e**)**.**

Total cell wall fluorescence of now-dead prey cells (TADA) showed no appreciable change through the invasive process (**Supplementary Figure 1**); however, both labelling patterns and signal intensities of pulsed HADA fluorescence showed dramatic differences depending on the stage of predation.

HADA pulses early in the infection, 15 or 30 min post-mixing of predators with prey resulted in labelling of various sub-cellular features. In particular, intense, localised, focal HADA marks on the prey PG (and a gradient of HADA signal from that focal point) were seen associated with attached *B. bacteriovorus* cells revealing the entry point of the *B. bacteriovorus* during the earliest predator-prey interaction (**Figure 1f**).

In order to further characterize these sub-cellular features in early predation, we imaged these labelled cells with high resolution 3D Structured Illumination Microscopy (3D-SIM). 3D-SIM resolved most of these focal marks of HADA labelling as annular ring structures (~25% of all HADA-bright prey cells investigated at earliest predation point, **Figure 2**, **Supplementary Table 2 and Supplementary Movie 1**) having a width (~0.24 µm; **Supplementary Table 2**) slightly less than that of a *B. bacteriovorus* cell (~ 0.33 µm) at the point of predator invasive cell pole : prey contact. This is consistent with the *B. bacteriovorus* 'squeezing through the entry pore' idea suggested by electron micrographs in earlier work[16,21,22]. Therefore, these HADA foci likely indicate the specific modification of the prey cell wall by predator during entry

(**Figure 2a**). The ring of HADA modification was on the prey PG rather than the predator PG, as it was always observed at the point of the prey PG, whether the predator was on the outside, inside, or partially entering the prey cell (**Supplementary Figure 2 a-c**). Furthermore, rare instances were observed where the predator had become detached from the prey but the HADA foci were still visible, confirming that these foci were indeed on the prey PG (**Supplementary Figure 2d**).

To establish that the dark channel in the HADA focal mark was indeed an entry pore in the prey PG we needed to detect the reduction of prey-PG material at the HADA channel centre. Using a more outer-membrane permeable *E. coli imp4213*$^{-}$ mutant strain as an alternative prey allowed us to label the prey PG uniformly and more completely with otherwise poorly outer-membrane permeable TADA[9]. In these cells, dark pores in the TADA signal (arrowheads TADA channel **Figure 3a**) were present, coincident with, and central within, the HADA ring (**Figure 3a** and **Supplementary Table 3**). These results represent a direct observation of *B. bacteriovorus* generating a ringed pore in the prey PG; a process that had previously been only inferred from indirect evidence[16,22,23].

Our approach also allowed us to distinguish clear deformations of the prey cell wall at the point where the *B. bacteriovorus* cell had entered (arrowheads, **Figure 2b**, arrowheads HADA channel **Supplementary Figure 3** and **Supplementary Table 2**) clarifying visually previous suggestions that *B. bacteriovorus* enzymatic modifications of prey cell walls may act to soften them[18,24].

To investigate dynamic changes in pores after invasion, we analysed (**Supplementary Table 2, Figure 2c** and **Supplementary Figure 2e**), ~400 HADA labelled *E. coli* S17-1 bdelloplasts. In 27% of these containing <u>internalised</u> *B. bacteriovorus* there was a HADA ring similar to the entry pore on bdelloplasts, located at the prey-predator contact point on the prey wall-proximal pole of the internalised *B. bacteriovorus* cells (red arrowheads, **Supplementary Figure 2e** and **Supplementary Table 2).** In some cases (4%) the HADA patches were filled discs (white arrowheads **Figure 2c** and yellow arrowheads **Supplementary Figure 2e).** Such discs were

also coincident with dark pores in TADA label of *E. coli imp4213* mutant bdelloplasts **(Figure 3c** and **Supplementary Table 3)** suggesting that they are sealing discs made by internalised *B. bacteriovorus* to close the prey, keeping the bdelloplast intact for predator consumption of contents.

### ***B. bacteriovorus*** **establishment inside prey is accompanied by an L,D-transpeptidase-mediated prey wall modification**

As the *B. bacteriovorus* cells enter the prey periplasm, the prey cells become rounded (**Figure 2a**), forming a bdelloplast[13]. During this period, the extent of HADA incorporation to the whole rounding wall of the (now dead) prey substantially increased and peaked around 45 min post-mixing, with ~2 to 4 times more HADA signal-intensity (blue line, **Figure 4a,** see methods for details) than the mean HADA labelling at later 2, 3, and 4 hour predation time points.

Previous global transcriptomic work had shown that the predicted *B. bacteriovorus* L,D-transpeptidase (Ldt) genes, *bd0886* and *bd1176,* are transcriptionally upregulated at 30 minutes from the start of predation about fivefold and sixfold, respectively[25]. These predicted L,D-transpeptidases, therefore, are good candidates for prey wall modification enzymes during bdelloplast establishment. Reverse transcription-PCR analysis confirmed that the expression of both genes peaked at 15-30 minutes into predation (**Figure 4b**); time points at which HADA incorporation to the prey walls begins (blue line, **Figure 4a**). Deletion of both of these *ldt* genes (leaving 17 $ldt_{Bd}$ genes intact) resulted in a Δ*bd0886*Δ*bd1176* predator (named Δ*2ldt*) that caused ~2-4 times less prey HADA incorporation activity than the wild type (blue line vs. orange line, **Figure 4a** and representative images in **Figure 4c** vs. **Figure 4d**). This significant difference suggests that these two *B. bacteriovorus ldt* gene products are responsible for the majority of the overall HADA pulse incorporation into prey wall within the first 2 hours of predation. A C-terminal fusion of mCherry to one of these two Ldts (Bd1176) localized to the prey bdelloplast, suggesting that this transpeptidase was exported from predator to bdelloplast and so was acting on the prey PG (**Supplementary Figure 4**).

**Bdelloplast wall modification is largely by the action of *B. bacteriovorus* enzymes which act upon uncrosslinked tetrapeptides of the prey PG**

In order to test the nature of the bdelloplast wall modification, we quantified HADA incorporation in bdelloplasts formed by *B. bacteriovorus* predation on different *E. coli* prey lacking different PG modification functionalities. The prey strain *E. coli* BW25113 Δ6LDT lacks all of the 6 *E. coli* L,D-transpeptidases (and therefore any L,D-transpeptidation activity). It lacks tripeptides, 3-3 crosslinks and PG-attached Lpp, and is rich in tetrapeptides[26,27]. The prey strain *E. coli* BW25113 ΔdacA lacks the major *E. coli* D,D-carboxypeptidase DacA and so contains more pentapeptides in its PG. The prey strain *E. coli* BW25113 Δ6LDTΔdacA lacks all 6 L,D-transpeptidases and the D,D-carboxypeptidase DacA and so contains mainly tetrapeptides, some pentapeptides, and lacks the modifications introduced by L,D-transpeptidases. Compared to the wild type prey strain *E. coli* BW25113 wt, predation of these strains by *B. bacteriovorus* and pulse labelling with HADA at 35-45 minutes post mixing of predator and prey, resulted in significantly more HADA incorporation for both prey strains lacking the L,D-transpeptidase activity (Δ6LDT and Δ6LDT ΔdacA, **Figure 5a**), but with no significant difference for prey lacking DacA alone (**Figure 5a**). In the absence of *B. bacteriovorus* predation, prey cells in Ca/HEPES buffer pulsed with HADA showed a fraction of the HADA incorporation when compared to the prey strains subjected to *B. bacteriovorus* predation (~1.5-14.6% of HADA incorporation, controls versus +Bds, **Figure 5a**). The majority of the *E. coli* self-labelling (in controls in the absence of *B. bacteriovorus* **Figure 5a**) was absent in the *E. coli* BW25113 Δ6LDT showing the $Ldt_{EC}$ to be responsible for this small amount of labelling. That predation of this strain actually resulted in more HADA incorporation further supports the notion that this incorporation is by *Bdellovibrio* encoded enzymes rather than those of the prey. Altogether, these results suggest that a significant proportion of the strong HADA incorporation observed on the prey PG during predation involves predator L,D-transpeptidase activity on tetrapeptides of the prey bdelloplast PG (and not D,D-transpeptidase activity on pentapeptides). These data, along with Bd1176-mCherry and Δ*2ldt*

data above, show that this activity comes from L,D-transpeptidases secreted by the *B. bacteriovorus* and not due to lingering activities of prey Ldt enzymes.

**L,D-Transpeptidase$_{Bd}$ -mediated prey wall modification confers bdelloplast physical robustness**

To determine the role of the L,D-transpeptidase activity, we assayed the stability of bdelloplasts produced by wild type *B. bacteriovorus* or by Δ*2ldt* mutant predator under osmotic challenge using the β-galatosidase substrate chlorophenyl red-β-D-galactopyranoside (CPRG) method to screen for damage to bacterial cell walls[28].

Bdelloplasts, at the peak of Ldt FDAA transfer- 1 hour post-synchronous infection of *E. coli* S17-1 (*lac*$^+$) prey; were subjected to osmotic upshock or downshock[29]. We observed increased β-galactosidase activity (Figure 5b) in the supernatant from shocked bdelloplasts formed by Δ*2ldt* mutant predators relative to wild-type in all conditions tested, including a small but significant) increase in levels from bdelloplasts formed by Δ*2ldt* predators, only subjected to the stress of centrifugation and resuspension in buffer (**Figure 5b**). These data suggest that Bd0886 and Bd1176 L,D-transpeptidase activities strengthen the bdelloplast wall to resist bursting during periods of *B. bacteriovorus* predatory intra-bacterial growth, after prey-entry.

To investigate if this Ldt modification had any effect on the bdelloplast morphology, we measured the sizes and shapes of the prey and bdelloplasts. Early bdelloplasts (45-60 minutes) formed by the Ldt mutant *B. bacteriovorus* were slightly, but significantly ($p$<0.0001) less round than those formed by the wild-type **(Supplementary Figure 5)**. We hypothesise that the less robust bdelloplasts formed by the Ldt mutant result in more flexible walls that warped more by the invading *B. bacteriovorus* cell, visible at the earlier stage of invasion after the *B. bacteriovorus* cell squeezed into the full prey cell. At later stages of invasion (2-4 hours) degradation of prey cell content may be why the differences between bdelloplasts formed by the mutant or the wild-type are no longer significant.

**Multi-coloured FDAA labelling provides direct evidence for the zonal mode of elongation and synchronous division of *B. bacteriovorus* growing inside prey**

*B. bacteriovorus* grow without binary fission, as a single multi-nucleoid filament inside prey[30]. At later timepoints, after 2 hours post-mixing, we observed filamentous cell elongation of the *B. bacteriovorus* within bdelloplasts (**Figure 6a**)[30]. Attack phase (AP) *B. bacteriovorus* were added in excess to ensure efficient predation in our experiments and AP predator cells that did not enter prey can be seen to retain substantial initial BADA labelling (**Figures 6a** and yellow arrowheads, **6b)**, because they do not replicate outside prey. On the other hand, after 2-3 hour post-mixing, we observe some green BADA transfer into the prey bdelloplast structure (BADA signal on bdelloplasts, **Figure 6a**) which may represent a predator-to-prey DAA turnover and transfer event as the growing *B. bacteriovorus* make new PG during elongation. While potentially fascinating, quantifying this inter-wall transfer proved impossible to resolve with current reagents. The high level of BADA accumulation in these bdelloplast walls appears to be more than could have been accrued from just one invading *Bdellovibrio*. This may be a slow accumulation into the prey PG of free BADA present in the medium. This BADA may have been released from excess non-invading *Bdellovibrio* due to their self-PG turnover, and/or releasing of BADA transiently accumulated in their cell envelopes. This pool of free BADA would be present throughout the 4 hour predatory cycle and so could incorporate into prey over a longer time compared to the 10 minute pulses of HADA availability.

3D-SIM imaging showed that *B. bacteriovorus* cells elongate along the filament with numerous, focused zones of growth (labelled with HADA, red arrowheads, **Figure 6b**) covering the entire cell surface except the apparently inert poles (preserving the original BADA signal, green arrowheads, **Figure 6b**). Later, around 3 hours post-mixing, new HADA incorporation appears as defined narrow foci along the filament (**Figure 6a** and red arrowheads **6c**), at points in *B. bacteriovorus* where new division septa would be expected to form synchronously[30]. After 4 hour post-mixing, these foci become the points of septum formation (**Figure 6a** and yellow arrowheads **6d**). Finally, newly released, attack phase *B.*

*bacteriovorus* daughter cells (white arrowheads, **Figure 6d**) incorporate pulsed HADA all over the cell and can therefore be distinguished from excess BADA labelled predators that didn't enter prey cells by the presence of a strong HADA fluorescent signal, but low BADA fluorescent signal.

## Discussion

Here, using multi coloured FDAA labelling and super-resolution imaging, we directly visualise sub-cellular modifications by *B. bacteriovorus* on *E. coli* PG cell walls and their effects during predation. Our data define an entry port structure by which a *B. bacteriovorus* cell accesses the cytoplasmic membrane face of the prey cell wall and seals itself in. We also show the sites of PG growth in the non-binary fission mode of predator growth. In addition, we show that L,D-transpeptidase enzymes from the *B. bacteriovorus* modify the PG of prey during residency of the predator to establish a stable intracellular niche.

Pioneering enzymology of prey bdelloplast extracts in the 1970s had detected bulk enzyme activities suggestive of extensive predator-modification of prey PG. These included solubilisation of 25% of the *meso*-diaminopimelic acid (*m*-DAP) residues on the PG[23] and the addition of free *m*-DAP back to the bdelloplast[31]. *m*-DAP is a residue native to PG that has both L- and D- amino acid properties. Therefore, we see FDAAs in our studies acting as visible substrates for these enzymatic, fresco-like changes to the walls of invaded prey caused by *B. bacteriovorus* enzymes. Indeed, we show the *B. bacteriovorus*-facilitated, localised breakdown of the prey wall to form a pore, its re-sealing while also rounding the prey cell wall to form an osmotically stable bdelloplast.

The initial ring of intense FDAA incorporation matches with the gap on the prey cell wall at the contact point with the *B. bacteriovorus* pole (**Supplementary Tables 2** and **3, Figures 2a** and **3a)**. Such a re-modelling of the prey PG likely strengthens the predator entry point. We show also here (**Figures 2c** and **3b**) that such entry ports have accumulated centralised FDAA signal after *B. bacteriovorus* entry which might represent a gradual ring-to-disc re-sealing

activity of this pore; a process which had previously been only inferred by indirect evidence of "scars" left behind on the prey cell wall at the point of entry[32].

The most extensive prey cell wall modification occurs 30-45 min after mixing *B. bacteriovorus* with the prey; involving the L,D-transpeptidases with major contributions from 2 of the 19 $Ldt_{Bd}$ enzymes encoded by genes *bd0886* and *bd1176* (**Figure 4a**). These observations may be due to pulsed FDAAs mimicking the incorporation of previously solubilised *m*-DAP reported in early *B. bacteriovorus* studies[23,31] but this is beyond our present experimentation. While we were able to isolate fluorescent FDAA labelled sacculi, amounts were not sufficient for mass spectrometry-based identification of sites of D-amino acid incorporation in *Bdellovibrio* or *E. coli* (**Supplementary Figure 7**). Incorporation of non-canonical D-amino acids into the cell wall is a stress response in *Vibrio cholerae*, which is shown to stabilize the PG integrity of the cells in stationary phase[2]. The incorporation of native *m*-DAP[31] and/or D-amino acids into the prey cell wall by *B. bacteriovorus* Ldts early in the predation (15 min – 1 hour) could represent an analogous means of forming a stabilised and stress resistant bdelloplast. The susceptibility of bdelloplasts formed by the *Δ2ldt* mutant predator to bursting during osmotic stress (**Figure 5b**) supports this hypothesis.

FDAA labelling also elucidated the growth of the intraperiplasmic *B. bacteriovorus* predator directly (**Figure 6**). Growth starts in patches along the length of the *B. bacteriovorus* cell, but not at the poles (**Figure 6a** and **6b**). After *B. bacteriovorus* septation, final predator self PG modification produces attack phase *B. bacteriovorus* (**Figure 6d**) which each emerge with one flagellated and one piliated pole[21,33]. These experiments provide evidence that both predator poles can carry out bilateral growth, along the length of the cell, rather than one "old" pole remaining attached to the membrane and growth emanating solely from specific regions[30,34]. Synchronous septum construction (that results in odd or even progeny numbers) is seen along the length of the filamentous *B. bacteriovorus* growing within the bdelloplast (**Figures 6a, 6c-d**), confirming earlier movies of this synchronous division[30].

In conclusion, the ability to distinctly label the PG containing cell walls of two different genera of interacting bacteria with different coloured FDAAs, has illuminated a series of dynamic molecular modifications that predatory *B. bacteriovorus* make to prey-cell walls and self-cell walls during their intraperiplasmic lifestyle. These modifications (pore formation and resealing without bacterial bursting and PG remodelling with free small molecules, i.e. DAAs, in dual cell systems) are previously uncharacterised in bacteria, and are key mechanisms of *B. bacteriovorus* predation. Given the inherent promiscuity of virtually all PG containing bacteria to incorporate FDAAs *in situ*[9,35] we expect this general approach to be helpful for visualising interactions of other complex bacterial communities, e.g. microbiota. Accordingly, we would not be surprised if this and similar approaches illuminate other examples of inter-generic PG modifications with novel functions.

**Correspondence**

Correspondence and requests for materials should be addressed to R. Elizabeth Sockett.

**Competing Financial interests**

The authors declare that there are no competing financial interests.

**Acknowledgements**

We thank Dr Daniel Kearns and his laboratory (Indiana University, USA) for facilities and hospitality to culture *B. bacteriovorus*, Dr Andrew Lovering (University of Birmingham UK) for insights and assistance with the alignment of L,D-transpeptidase protein sequences in *B. bacteriovorus*, Dr Teuta Pilizota (University of Edinburgh UK) for advice on osmotic stress conditions, Dr Rebecca Lowry (University of Nottingham) for assistance in image acquisition. This work was supported by BBSRC grant [BB/M010325/1] for CL and by a Leverhulme Trust (UK) Research Leave Fellowship RF-2013-348 to RES, NIH GM113172 grant to M.V.N. and Y.V.B. and R35GM122556 and GM51986 to Y.V.B. AD was supported by an EMBO long term fellowship, WV by funds from the Wellcome Trust (101824/Z/13/Z).

## Author Contributions

EK and RES conceived the study and carried out the experiments along with CL using reagents constructed by MvN and JR, and bacterial strains constructed by RT and ADe. JG and JB performed muropeptide analysis in WV's lab. ADu wrote code and aided CL and EK with image analysis. YB provided microscopy facilities and with MvN and WV provided helpful comments. EK, CL and RES wrote the manuscript with inputs and comments from the other authors.

## Figures

**Figure 1** Background and introduction to experimental procedures.

**a-** Biosynthesis of PG starts in the cytoplasm by sequential addition of L-Ala, D-Glu, a diamino acid and a dipeptide of D-Ala-D-Ala to disaccharide units. This subunit is then incorporated into the murein sacculus by glycan polymerisation via transglycosylases. The D-Ala at position 5 can also be cleaved by the actions of D,D-carboxypeptidases. **b-** L,D-transpeptidases cleave the D-Ala from position 4 and utilise the energy from cleaving this bond to form a 3-3 crosslink with another acyl-acceptor stem peptide or replace the D-Ala with a free D-amino acid such as fluorescent D-amino acids (FDAAs). **c -** Timed stages of the predatory cycle of *B. bacteriovorus* (black) bacteria invading *E. coli* prey (gray). 0-15 minutes post-mixing of *B. bacteriovorus* and prey; *B. bacteriovorus* attach and begin to enter the outer layers of the prey. 30 minutes; most of the *B. bacteriovorus* have entered the prey periplasm, modifying the prey cell to form a rounded "bdelloplast". 1-3 hours; *B. bacteriovorus* growth occurs at the expense of the prey cell contents in the form of elongation as a filament. 4 hours; this filament fragments into smaller attack phase cells which break out from the bdelloplast **d-** FDAAs used in this study, colours are representative of emission maxima. **e-** Multi-coloured FDAA labelling scheme with time points observed by wide field epifluorescence microscopy. Predator and prey cells were pre-labelled separately with BADA and TADA respectively before being washed and then mixed. Samples of this mixed infection were then pulse-labelled with HADA

for 10 minutes before each time point before being fixed, washed, then microscopically observed. **f-** Phase contrast and epi-fluorescent microscopy images of the early stages of *B. bacteriovorus* predation The *B. bacteriovorus* are false-coloured in green, the *E. coli* prey cells are false-coloured in red and pulsed HADA signal is false-coloured in blue. Each channel is displayed independently in white and with all 3 fluorescence channels merged in epifluorescence (EPI) overlay. HADA fluorescence signal on the prey wall has an intense focus at each point of *B. bacteriovorus* contact and spreads from this point across the rest of the wall. Scale bars, 1 µm. The two images are representative of between 321 and 10,546 cells for each timepoint, detailed in **Supplementary Table 1**.

**Figure 2**- 3D-SIM images of early predation by *B. bacteriovorus* (pre-labelled with BADA, false-coloured red) on prey *E. coli* cells after a pulse labelling for 10 minutes with HADA (false-coloured cyan) to show early modification of cell walls.

**a-** Predation 15 minutes post mixing reveals a ring of HADA-labelled prey cell wall modification at the point of *B. bacteriovorus* contact (arrowheads) and of similar width to the *B. bacteriovorus* cell (see **Supplementary Table 2**) . Central pores in the labelled PG material can be seen where the *B. bacteriovorus* image is artificially removed from the overlay of the two channels. Such annuli may represent a thickened ring of PG modification. In the white inset; the lookup table for the BADA channel has been separately adjusted until all the BADA labelled predators were clearly visible. Three representative examples are displayed. **b-** Prey PG is deformed around the site of *B. bacteriovorus* invasion (arrowheads). **c-** The cells show HADA fluorescence at the end of the internal *B. bacteriovorus* cell (arrowheads) which likely represents transpeptidase activity re-sealing the hole in the prey PG after the *B. bacteriovorus* cell has entered. Images are representative of >100 3D-reconstructed cells in two independent experiments (**Supplementary Table 2** for details of numbers analysed). Scale bars are 1µm.

**Figure 3-** 3D-SIM images of early predation by *B. bacteriovorus* (pre-labelled with BADA, false-coloured green) on prey *E. coli imp4213* cells (which are more permeable and thus

susceptible to the TADA pre-labelling, false coloured in red) after a pulse labelling for 10 minutes with HADA (false-coloured cyan) to show early modification of cell walls.

**a-** FDAA labelling scheme (using excess *B. bacteriovorus* to promote synchronous invasion of *E. coli* Δ*imp4213* mutant prey) with time points observed by 3D-SIM fluorescence microscopy. Predator and prey cells were pre-labelled separately with BADA and TADA respectively before being washed and then mixed. Samples of the mixed infection were then pulse-labelled with HADA for 10 minutes before time points up to 30 minutes, the cells were fixed, washed and then microscopically observed. **b-** Predation 30 minutes post mixing with this prey strain reveals a pore in the TADA signal coincident with the ring of HADA-labelled prey cell wall modification at the point of *B. bacteriovorus* contact (arrowheads) and of similar width to the *B. bacteriovorus* cell (**Supplementary Table 3**) . **c-** In several cases (**Supplementary Table 3**) where the *B. bacteriovorus* cell had entered into the prey cell and established itself in the periplasm of the bdelloplast, the pore in the TADA was coincident with a patch of HADA- and thus is likely to represent the sealing of the pore through which the *B. bacteriovorus* had entered. Images are representative of two independent experimental repeats. Scale bars are 1 µm.

**Figure 4** Quantitative and qualitative effects of two L,D-transpeptidases on prey cell wall modifications by FDAAs and their expression profiles.

**a**- Plot of mean HADA fluorescent signal of cells against time throughout the predation cycle. Measurements are total mean background-corrected fluorescent signal from wild type *B. bacteriovorus* cells (grey line), *Δ2ldt* mutant (yellow line), or invaded prey bdelloplast. Mean fluorescent signal was significantly lower in the bdelloplasts invaded by the *Δ2ldt* mutant (orange line) compared to those invaded by the wild type (blue line). Time is in minutes post-mixing of predator and prey and fluorescence is in relative fluorescent units. Data were from at least two independent repeats (see **Supplementary Table 1** for details of n). Error bars are SEM. The HADA signal differences between *E. coli* preyed upon by wt or *Δ2ldt* mutant

were significant in each of the time points ($p$<0.0001 **** for all time points except 240 min, for which $p$=0.016 * by the Mann-Whitney test)

**b-** RT-PCR showing the expression of predicted L,D-transpeptidase genes *bd0886* and *bd1176* or control gene *dnaK*, over the predatory cycle of *B. bacteriovorus*. . L = 100bp DNA ladder, AP = Attack Phase cells, 15-45, 1h-4h = minutes or hours respectively since mixing of *B. bacteriovorus* and prey. Ec = *E. coli* S17-1 RNA (negative control: no *B. bacteriovorus*); NT = no RNA control; Gen = *B. bacteriovorus* HD100 genomic DNA (positive control). The cartoon above represents the different stages of predation. Expression of both genes peaked at 15-30 minutes post-mixing predator and prey. Two independent repeats were carried out and showed the same transcription pattern.

**c-** FDAA labelling of *B. bacteriovorus* wild-type HD100 and **d-** Δ*2ldt* mutant predation and bdelloplast establishment. White arrowheads point to HADA modification of the bdelloplast and HADA polar foci visible on the mutant predators inside the bdelloplast. The *B. bacteriovorus* are false-coloured green, the *E. coli* prey cells are false-coloured red and the HADA pulse-labelling is false-coloured blue. HADA fluorescence of the prey cell during predation with the L,D-transpeptidase mutant is less than for predation by the wild-type. Scale bars are 1 µm. Images are representative of 5 independent replicates for the wild-type and 2 independent replicates for the *Δ2ldt* mutant (**Supplementary Table 1** for details of n).

**Figure 5** Plots showing HADA incorporation in the PG of prey *E. coli* mutants upon *B. bacteriovorus* predation and showing the damage by osmotic shock to bdelloplasts formed by *B. bacteriovorus* Ldt mutants.

**a-** Chart of mean HADA fluorescent signal of prey strains preyed upon by *B. bacteriovorus* (+Bd), and pulsed with HADA at 35-45 minutes post mixing (the timepoint of maximal HADA incorporation for *E. coli* S17-1). Controls were in Ca/HEPES buffer without *B. bacteriovorus* predation, but pulsed with HADA at the same timepoint. Measurements are total mean background corrected fluorescent signal of prey cells and is reported in relative fluorescent

units measured by MicrobeJ. Prey cells lacking all 6 L,D-transpeptidases (Δ6LDT) accumulated more HADA fluorescence upon predation by *B. bacteriovorus*. Control samples without *B. bacteriovorus* predation accumulated considerably less HADA fluorescence. Controls of Δ6LDT prey cells without *Bdellovibrio* predation accumulated negligible HADA fluorescence. Data were from two (for the controls) or three independent repeats. Error bars are standard error of the means. WT- *E. coli* BW25113 wild-type strain YB7421, 6LDT- *E. coli* BW25113 Δ6LDT strain deficient in all 6 L,D transpeptidases, dacA- *E. coli* BW25113 strain YB7423 deficient in DacA, 6LDTdacA- *E. coli* BW25113 Δ6LDTΔ*dacA* strain YB7439 deficient in all 6 L,D transpeptidases and dacA. N/S- not significant; all other comparisons were significant $p<0.0001$, with the one exception shown, by the Mann-Whitney test.

**b-** CPRG β-galactosidase assay measuring cytoplasmic leakage of shocked *E. coli* bdelloplasts formed by wild type (BP HD100 WT) or bdelloplasts formed by *Δ2ldt* mutant *B. bacteriovorus* (BP Ldt- mutant) with controls of uninvaded *E. coli* prey cells (S17-1 only) or *B. bacteriovorus* cells alone (HD100 WT only). Red colour from positive CPRG reaction was measured by spectrophotometry at 574 nm and readings were normalised to each experiment. Bdelloplasts were harvested by centrifugation and shocked by resuspension in Ca/HEPES buffer for no shock- except centrifugation only (Buffer), Ca/HEPES buffer supplemented with 750mM NaCl (Upshock) or upshock followed by further centrifugation and resuspension in water (Downshock). Error bars are standard error of the mean. Statistical significance was determined by Student's *t*-test (2-tailed) $*p<0.05$ $**p<0.01$ $***p<0.001$. Data were the mean of 7 independent repeats.

**Figure 6-** Epifluorescence and 3D-SIM images of the later stages of predation to show PG modification of the growing internal *B. bacteriovorus*.

**a-d,** Phase contrast (**a**) and epi-fluorescent microscopy and 3D-SIM (**b-d**) images of the later stages of *B. bacteriovorus* predation (after the peak of bdelloplast HADA labelling, by wild type predator, has ended). The *B. bacteriovorus* were pre-labelled with BADA and are false-coloured in green, the *E. coli* prey cells were pre-labelled with TADA and are false-coloured

in red. The cells were pulse-labelled for 10 minutes before each acquisition timepoint with HADA, which is false-coloured in cyan. Each channel is displayed independently and with all 3 fluorescence channels merged. The HADA fluorescence indicates synthesis of the *B. bacteriovorus* PG, which initiates at many points along the growing predator (2 hours, **b;** red arrowheads) except the poles (2 hours; **b**; green arrowheads), before developing into foci (3 hours; **c**; red arrowheads), which become septa (4 hours; **d**, red arrowhead). After division, newly released *B. bacteriovorus* can be seen to modify their whole PG (4 hours; **d**, white arrowheads). *B. bacteriovorus* that did not invade (there was an excess of *B. bacteriovorus* to ensure efficient predation) can be seen to have a strong BADA signal and low HADA signal (4 hours; **d**, yellow arrowheads). Images are representative examples from thousands of cells from five independent experiments (**a**) and of >100 3D-reconstructed cells in two independent experiments (**b-d**) see **Supplementary Table 1** for numbers of cells analysed. Scale bars are 1µm.

## Materials and Methods

### RNA isolation from predatory cycle and RT-PCR analysis

Synchronous predatory infections of *B. bacteriovorus* HD100 on *E. coli* S17-1 in Ca/HEPES buffer (2 mM $CaCl_2$ 25 mM HEPES pH7.6), or strain S17-1 suspended in Ca/HEPES alone, were set up as previously described[36] with samples throughout the timecourse being taken and total RNA isolated from them. This semi-quantitative PCR allows the evaluation of specific predator transcripts in the presence of fluctuating levels of prey RNA as the predator degrades it. RNA was isolated from the samples using a Promega SV total RNA isolation kit with the RNA quality being verified by an Agilent Bioanalyser using the RNA Nano kit. RT-PCR was performed with the Qiagen One-step RT-PCR kit with the following reaction conditions: One cycle 50°C for 30 minutes, 95°C for 15 minutes, then 25 cycles of 94°C for 1 min, 50°C for 1 min, 72°C for 1 min, a 10 minutes extension at 72°C after the 30 cycles, and finally a 4°C hold. Two independent repeats were carried out. Primers to anneal to *bd0886* were 5'-AGCCTCTACATGGGTGCAAG -3' and 5'- AACTTGGCTGCATACCAACC -3'. Primers to

anneal to *bd1176* were 5'-GCCAACGCCAGCGTGAATGC-3' and 5'-GGCCGTCGTTGAGTTGCTGC-3'.

**Generating gene deletion mutants in *B. bacteriovorus***

Markerless deletion of both the *bd0886* and *bd1176* genes from *B. bacteriovorus* HD100 was achieved sequentially as described previously[18,37]. Primers designed to amplify to the upstream region of *bd0886* were: Bd0886F 5'-ACGGGGTACCCACGATCCCATCTTATAAGC -3' and

Delbd0886F 5'-GGAGATTATATGAAAGCTTTCTAGAATGGACTCTGTTCCTGCGC-3'. Primers designed to amplify to the downstream region of *bd0886* were:

Delbd0886R 5'-GCGCAGGAACAGAGTCCATTCTAGAAAGCTTTCATATAATCTCC-3' and

Bd0886R 5'-CTGTAGCATGCTTCAGATCCTCGCTGAAACC-3'

Primers designed to amplify to the upstream region of *bd1176* were: Bd1176-F 5'-GCGCAAAAGCTTTCGCAAGCTGGGTGTTCAGC -3' and

Delbd1176F 5'- GATTGCCAGCTCCCCTATGTCTAGAAATCCTCCGAAGATCGTTT -3'. Primers designed to amplify to the downstream region of *bd1176* were:

Delbd1176R 5'- AAACGATCTTCGGAGGATTTCTAGACATAGGGGAGCTGGCAATC -3' and

Bd1176-R 5'- ACGGGGTACCGGATGTGATTCATACCAGCC-3'

**Construction of an *E. coli* strain lacking all 6 LD-transpeptidases**

*E. coli* BW25113Δ6LDT lacks all five previously published LD-transpeptidase genes (*erfK*, *ybiS*, *ycfS*, *ynhG*, *ycbB*)[27,38] plus a sixth gene encoding a putative LD-transpeptidase, *yafK*. Gene deletions were generated and combined by transferring *kan*-marked alleles from the Keio *E. coli* single-gene knockout library[39] into relevant background strains using P1 phage transduction[40]. The Keio pKD13-derived *kan* cassette is flanked by FRT sites, allowing removal of the *kan* marker via expression of FLP recombinase from plasmid pCP20 to generate unmarked deletions with a FRT-site scar sequence[39,41]. The gene deletions present in BW25113Δ6LDT were verified by PCR, and the analysis of the PG composition showed

that muropeptides generated by the activities LD-transpeptidases were below the limit of detection.

**Fluorescent tagging of Bd1176**

The *bd1176* gene lacking its stop codon was cloned into the conjugable vector pK18*mobsacB* in such a way as to fuse the gene at the C-terminus with the mCherry gene. This fusion was introduced into *B. bacteriovorus* by conjugation as described previously[42]. Cloning was carried out using the NEB Gibson cloning assembly kit and the primers used (5'-3') were: cgttgtaaaacgacggccagtgccaATGACAAAGATTAATACGCGCC, ccttgctcaccatGTTGTTGCCGCCTCTTCTTG, aggcggcaacaacATGGTGAGCAAGGGCGAG and cagctatgaccatgattacgTTACTTGTACAGCTCGTCCATGCC Epi-fluorescence microscopy was undertaken using a Nikon Eclipse E600 through a 100x objective (NA 1.25) and acquired using a Hammamatsu Orca ER Camera. Images were captured using Simple PCI software (version 6.6). An hcRED filter block (excitation: 550-600 nm; emission: 610-665 nm) was used for visualisation of mCherry tags.

**Labelling of cells with FDAAs and imaging**

*Bdellovibrio bacteriovorus* HD100 cells were grown predatorily for 16 hours at $30^0$C on stationary phase *E. coli* S17-1 prey, until these were lysed. The *B. bacteriovorus* were then filtered through a 0.45 µm filter (yielding ~2 x $10^8$ pfu per ml) and concentrated 30 x by centrifugation at 12,000 x *g* for 5 minutes. The resulting pellet was resuspended in Ca/HEPES buffer, (2 mM $CaCl_2$ 25 mM HEPES ph7.6) and then pre-labelled with a final concentration of 500 µM BADA (by addition of 5 µl of a 50 mM stock in DMSO) for 30 minutes at $30^0$C. The cells were then washed twice in Ca/HEPES buffer before being resuspended in an equal volume of Ca/HEPES buffer. *E. coli* S17-1 or *E. coli imp4213* cells were grown for 16 hours in LB at $37^0$C with shaking at 100 rpm and were back diluted to $OD_{600}$ 1.0 in fresh LB, (yielding ~1 x $10^9$ cfu per ml) and labelled with final concentration of 500 µM TADA (by addition of 5 µl of a 50 mM stock in DMSO) for 30 minutes at $30^0$C, before being washed twice in Ca/HEPES

buffer then resuspended in an equal volume of Ca/HEPES buffer. *E. coli* BW25113 strains were grown as for strain S17-1, except strains YB7423, YB7424 and YB7439 were supplemented with 50 µg per ml kanamycin suphate for incubation and washed of this by centrifugation at 5,000 x *g* for 5 minutes, resuspension in an equal volume of LB broth and further centrifugation at 12,000 x *g* for 5 minutes before back-dilution to $OD_{600}$ 1.0 in Ca/HEPES buffer. This resulted in similar numbers of cells for each strain; *E. coli* BW25113 Δ6LDT $5.1 \times 10^8 \pm 3.6 \times 10^7$, YB7423 $5.2 \times 10^8 \pm 1.8 \times 10^8$, YB7424 $4.9 \times 10^8 \pm 2 \times 10^7$, YB74394.3 $\times 10^8 \pm 1.6 \times 10^8$ as determined by colony forming units.

Defined ratios of approximately 5 *B. bacteriovorus* predators to 1 *E. coli* prey were then prepared for semi-synchronous predation experiments to allow FDAA labelling of dynamic PG changes as the predators were invading and replicating within the prey. Five hundred microlitres of the pre-labelled *B. bacteriovorus* were mixed with 400 µl of the pre-labelled *E. coli* and 300 µl of Ca/HEPES buffer and incubated at $30^0$C. For HADA pulse-labelling, 120 µl samples of these predatory cultures were added to 1.2 µl of a 50 mM stock of HADA in DMSO 10 minutes before each sampling timepoint for microscopy and returned to $30^0$C incubation. These experimental timescales are consistent and shown in diagram above figures (for example 30 minute predation timepoint = 20 minutes of predator mixed with prey, plus 10 minutes of subsequent HADA labelling, followed by immediate fixation and then washing). At each timepoint, all the 120 µl predator-prey sample was transferred to 175 µl ice cold ethanol and incubated at $-20^0$C for at least 15 minutes to fix the cells. The cells were pelleted by centrifugation at 12,000 x *g* for 5 minutes, washed with 500 µl PBS and resuspended in 5 µl Slowfade (Molecular Probes Ltd) and stored at $-20^0$C before imaging. 2 µl samples were imaged using a Nikon Ti-E inverted fluorescence microscope equipped with a Plan Apo 60x/1.40 Oil Ph3 DM objective with 1.5x intermediate magnification, or a Plan Apo 100x/1.45 Ph3 objective, a CFP/YFP filter cube and an Andor DU885 EMCCD or an Andor Neo sCMOS camera using CFP settings for detection of HADA (emission maximum 450 nm), a FITC filter cube for detection of BADA (emission maximum 512 nm) and others (acquisition and image processing details in **Equipment and settings** in supporting online material). Later timepoints

were prepared with similar HADA pulses carried out on further samples of the continuing predator- prey culture which extended to 4 hours of incubation at $30^0$C; the point at which new *B. bacteriovorus* predators emerge from lysed *E. coli* prey.

**Super resolution microscopy**

3D Structured illumination microscopy was performed using a DeltaVision OMX Imaging System equipped with an Olympus UPlanSApo 100X/1.40 Oil PSF objective and a Photometrics Cascade II EMCCD camera. The samples were excited with lasers at 405 nm, 488 nm, 561 nm and the emission was detected through 419 nm-465 nm, 500 nm-550 nm, 609 nm-654 nm emission filters. The image processing was conducted by SoftWorx imaging software. Further image analysis and processing was conducted via ImageJ or Icy (http://www.bioimageanalysis.org/). Acquisition and image processing details are in **Equipment and settings** in supporting online material.

**Quantitation of fluorescent signal**

For quantitation of fluorescent signal, images were acquired as above, but with unvarying exposure and gain settings. The exposures were chosen to give values that did not exceed the maximum so that saturation was not reached for any of the fluorescent channels. Images were analysed using the MicrobeJ plugin for the ImageJ (FIJI distribution) software (http://www.indiana.edu/~microbej/index.html)[43] which automates detection of bacteria within an image. The *E. coli* prey cells and *Bdellovibrio* cells were detected using the resulting binary mask from both the phase contrast and either the TADA or the BADA channels respectively. The *E. coli* prey cells and *B. bacteriovorus* cells were differentiated by defining two cell types based on size; Cell Type 1 (for *E. coli*) were defined by area 0.9-6 $\mu m^2$, length 1.5-7 µm, width 0.4-3 µm and all other parameters as default; Cell Type 2 (for the smaller *B. bacteriovorus* cells) were defined by area 0-1 $\mu m^2$, length 0.5-1.5 µm, width 0.2-0.8 µm and all other parameters as default. Manual inspection of the analysed images confirmed that the vast majority of cells were correctly assigned. *Bdellovibrio* cells were linked hierarchically with the *E. coli* prey cells, in order to distinguish between internalized, attached and unattached predator cells. The shape measurements including the angularity, area, aspect

ratio, circularity, curvature, length, roundness, sinuosity, solidity and width were measured for each type of cell. Background-corrected mean fluorescent intensity was measured for each cell and then the mean of these measurements was determined for each cell type, for each independent experiment. Typically, 500-5,000 cells were measured at each timepoint for each independent experiment (details of n for each sample in each experiment are presented in **Supplementary Table 1**).

**Code availability**

The images and the data were analyzed by MicrobeJ (5.11v), a freely available and open-source software. The code source is available upon request from Adrien Ducret.

**CPRG assay of leakage of osmotically shocked bdelloplasts derived from predation by Ldt mutant versus wild type *B. bacteriovorus.***

To evaluate whether DAA transfer to prey bdelloplast cell walls altered the physical stability of those walls to osmotic changes, an assay for leakage of cytoplasmic contents, including β-galactosidase was used, with the CPRG as a detection reagent.

*E. coli* S17-1 (*lac*$^+$) prey cells were grown for 16 hours in YT broth at 37°C with 200 rpm shaking, before being supplemented with 200 µgml$^{-1}$ IPTG for 2 hours to induce expression of *lacZ.* These prey cells were then centrifuged at 5,100 x *g* for 5 minutes and resuspended in Ca/HEPES buffer (2 mM $CaCl_2$ 25 mM HEPES ph7.6) then diluted to $OD_{600}$ 1.0 in Ca/HEPES buffer. *Bdellovibrio bacteriovorus* HD100 or *Δ2ldt* strains were grown predatorily for 16 hours at 29$^0$C on stationary phase *E. coli* S17-1 prey until these were fully lysed, and then *B. bacteriovorus* were filtered through a 0.45 µm filter, concentrated 50 x by centrifugation at 5,100 x *g* for 20 minutes and resuspended in Ca/HEPES buffer. Total protein concentration of these concentrated suspensions was determined by Lowry assay, and matched amounts of 50 µg of each strain were used for semi-synchronous infections (between 115 and 284 µl of concentrated suspension made up to a total of 800 µl in Ca/HEPES buffer) with 400 µl of diluted *E. coli* S17-1 prey cells. This resulted in a multiplicity of infection (MOI of *B.*

*bacteriovorus* cells : *E. coli* cells) of 1.4 to 10.5 for the wild-type strain HD100 as determined by plaque assay. The excess of predators resulted in >99.4% of *E.coli* prey cells rounded by invasion of strain HD100 and >99.6% of prey cells rounded by invasion of *Δ2ldt* mutant after incubation at 29°C for 1 hour with shaking at 200 rpm.

A control of prey only (400 µl diluted prey cells with 800 µl Ca/HEPES buffer) resulted in no rounded prey cells and a control of wild-type *B. bacteriovorus* HD100 cells only (50 µg in a total of 1200 µl Ca/HEPES buffer) was included. After incubation, bdelloplasts (or cells in the controls) were harvested by centrifugation at 17,000 x *g* for 2 minutes and supernatant removed. The pellets were resuspended in: 1) Ca/HEPES buffer supplemented with 20 $\mu gml^{-1}$ CPRG (Sigma) for centrifugation shock only 2) Ca/HEPES buffer supplemented with 750mM NaCl and 20 $\mu gml^{-1}$ CPRG for upshock 3) Ca/HEPES buffer supplemented with 750mM NaCl, incubated for 30 minutes at 29°C followed by centrifugation at 17,000 x *g* for 2 minutes and supernatant removed, then the pellet resuspended in water supplemented with 20 $\mu gml^{-1}$ CPRG for downshock. These were then incubated for 30 minutes at 29°C before purifying the supernatant, containing any bdelloplast leakage products, for β-galactosidase assay by removing cells by centrifugation at 17,000 x *g* for 2 minutes followed by filtration through a 0.2 µm filter. The β-galactosidase assay was carried out by incubation at 29°C for 26 hours and colour change was monitored by spectrophotometry at 574 nm. Data were normalised for each experiment.

Extra experimental considerations: The *Δ2ldt* mutant strain exhibited a plaquing phenotype, forming mostly very small plaques with ~1% forming larger plaques similar to the wild-type HD100 strain (see **Supplementary Figure 6**) and as such an accurate MOI could not be measured by plaques for this strain. To confirm that matching the input cells by Lowry assay resulted in similar numbers of *B. bacteriovorus*, and therefore a similar MOI, images of the mixed prey and predators were analysed. After the 1 hour incubation at 29°C, 40 µl samples were mixed with 2 µl of 0.3 µm polystyrene beads (Sigma; diluted 500 x and washed 5 x with water). 10 µl samples were dropped onto microscope slides with a 1% agarose pad made with

Ca/HEPES buffer and 20 fields of view were imaged at 1000 x phase contrast with a Nikon Ti-E inverted microscope. Images were analysed with the MicrobeJ plugin as described above, but including a third cell type definition for quantifying the beads defined by area 0-1, length 0.1-0.8, width 0.1-0.6 and all other parameters 0-max. This confirmed that there were not significantly different ratios of beads to *B. bacteriovorus* cells in the two strains (6.1 ± 3.9 for HD100, 6.9 ± 0.7 for *Δ2ldt* mutant) and that all visible prey cells were rounded up after 1 hour of incubation, indicating that an MOI of >1 was achieved (which was required for semi-synchronous infection). To confirm that the defective plaquing phenotype of the *Δ2ldt* mutant was not a result of low yield in liquid culture, images were analysed at the start and end of predatory growth in liquid. The average result of 5 Lowry assays was taken to match the starting amounts of *B. bacteriovorus*: 245 µl of strain HD100 and 337 µl of the *Δ2ldt* mutant strain (after filtration through a 0.45 µm filter, but not concentrated) were made up to 800 µl in Ca/HEPES buffer and added to 400 µl prey *E. coli* diluted to $OD_{600}$ 1.0 in Ca/HEPES buffer. This mix was imaged with beads as described above at time 0 and 24 hours (after incubation at 29°C with 200 rpm shaking) and analysed using the MicrobeJ plugin as described above. The increase in numbers of *B. bacteriovorus* cells per bead was not significantly different between the 2 strains (1.9 ± 0.5 for HD100 and 2.1 ± 0.8 for the *Δ2ldt* mutant). In both cases, the prey cells were almost eradicated after 24 hours with only 8-13 cells detected by MicrobeJ in the 20 fields of view for each experiment (reduced to 1.0 ± 0.4 % of starting values for HD100 and 3.3 ± 0.8 % for the *Δ2ldt* mutant).

## Data availability

The raw data that support the findings of this study are available from the corresponding author upon request.

## References

657 1 Mainardi, J. L. *et al.* A novel peptidoglycan cross-linking enzyme for a beta-lactam-resistant
658 transpeptidation pathway. *J Biol Chem* **280**, 38146-38152, doi:10.1074/jbc.M507384200
659 (2005).
660 2 Cava, F., de Pedro, M. A., Lam, H., Davis, B. M. & Waldor, M. K. Distinct pathways for
661 modification of the bacterial cell wall by non-canonical D-amino acids. *The EMBO Journal* **30**,
662 3442-3453, doi:10.1038/emboj.2011.246 (2011).
663 3 Magnet, S. *et al.* Specificity of L,D-transpeptidases from gram-positive bacteria producing
664 different peptidoglycan chemotypes. *J Biol Chem* **282**, 13151-13159,
665 doi:10.1074/jbc.M610911200 (2007).
666 4 Fura, J. M., Kearns, D. & Pires, M. M. D-amino acid probes for penicillin binding protein-
667 based bacterial surface labeling. *J Biol Chem* **290**, 30540-30550,
668 doi:10.1074/jbc.M115.683342 (2015).
669 5 Gupta, R. *et al.* The *Mycobacterium tuberculosis* protein LdtMt2 is a nonclassical
670 transpeptidase required for virulence and resistance to amoxicillin. *Nature medicine* **16**, 466-
671 469, doi:10.1038/nm.2120 (2010).
672 6 Peltier, J. *et al. Clostridium difficile* has an original peptidoglycan structure with a high level
673 of N-acetylglucosamine deacetylation and mainly 3-3 cross-links. *J Biol Chem* **286**, 29053-
674 29062, doi:10.1074/jbc.M111.259150 (2011).
675 7 Lam, H. *et al.* D-amino acids govern stationary phase cell wall remodeling in bacteria. *Science*
676 **325**, 1552-1555, doi:10.1126/science.1178123 (2009).
677 8 Radkov, A. D. & Moe, L. A. Bacterial synthesis of D-amino acids. *Appl Microbiol Biotechnol*
678 **98**, 5363-5374, doi:10.1007/s00253-014-5726-3 (2014).
679 9 Kuru, E., Tekkam, S., Hall, E., Brun, Y. V. & Van Nieuwenhze, M. S. Synthesis of fluorescent D-
680 amino acids and their use for probing peptidoglycan synthesis and bacterial growth in situ.
681 *Nature protocols* **10**, 33-52, doi:10.1038/nprot.2014.197 (2015).
682 10 Fleurie, A. *et al.* MapZ marks the division sites and positions FtsZ rings in *Streptococcus*
683 *pneumoniae*. *Nature* **516**, 259-262, doi:10.1038/nature13966 (2014).
684 11 Tsui, H. C. *et al.* Pbp2x localizes separately from Pbp2b and other peptidoglycan synthesis
685 proteins during later stages of cell division of D39. *Mol Microbiol* **94**, 21-40,
686 doi:10.1111/mmi.12745 (2014).
687 12 Pilhofer, M. *et al.* Discovery of chlamydial peptidoglycan reveals bacteria with murein sacculi
688 but without FtsZ. *Nature communications* **4**, 2856, doi:10.1038/ncomms3856 (2013).
689 13 Stolp, H. & Starr, M. P. *Bdellovibrio bacteriovorus* gen. et sp. n., a predatory, ectoparasitic,
690 and bacteriolytic microorganism. *Antonie van Leeuwenhoek Journal of Microbiology and*
691 *Seriology* **29**, 217-248 (1963).
692 14 Sockett, R. E. Predatory lifestyle of *Bdellovibrio bacteriovorus*. *Annu Rev Microbiol* **63**, 523-
693 539, doi:10.1146/annurev.micro.091208.073346 (2009).
694 15 Rittenberg, S. C. & Shilo, M. Early host damage in the infection cycle of *Bdellovibrio*
695 *bacteriovorus*. *J Bacteriol* **102**, 149-160 (1970).
696 16 Abram, D., Castro e Melo, J. & Chou, D. Penetration of *Bdellovibrio bacteriovorus* into host
697 cells. *J Bacteriol* **118**, 663-680 (1974).
698 17 Abram, D. & Davis, B. K. Structural properties and features of parasitic *Bdellovibrio*
699 *bacteriovorus*. *J Bacteriol* **104**, 948-965 (1970).
700 18 Lerner, T. R. *et al.* Specialized peptidoglycan hydrolases sculpt the intra-bacterial niche of
701 predatory *Bdellovibrio* and increase population fitness. *PLoS pathogens* **8**, e1002524,
702 doi:10.1371/journal.ppat.1002524 (2012).
703 19 Lambert, C. *et al.* Ankyrin-mediated self-protection during cell invasion by the bacterial
704 predator *Bdellovibrio bacteriovorus*. *Nature communications* **6**, 8884,
705 doi:10.1038/ncomms9884 (2015).

20 Lambert, C. *et al.* Interrupting peptidoglycan deacetylation during *Bdellovibrio* predator-prey interaction prevents ultimate destruction of prey wall, liberating bacterial-ghosts. *Sci Rep* **6**, 26010, doi:10.1038/srep26010 (2016).
21 Evans, K. J., Lambert, C. & Sockett, R. E. Predation by *Bdellovibrio bacteriovorus* HD100 requires type IV pili. *J Bacteriol* **189**, 4850-4859, doi:JB.01942-06 [pii]10.1128/JB.01942-06 (2007).
22 Koval, S. F. *et al. Bdellovibrio exovorus* sp. nov., a novel predator of *Caulobacter crescentus*. *Int J Syst Evol Microbiol* **63**, 146-151, doi:10.1099/ijs.0.039701-0 (2013).
23 Thomashow, M. F. & Rittenberg, S. C. Intraperiplasmic growth of *Bdellovibrio bacteriovorus* 109J: solubilization of *Escherichia coli* peptidoglycan. *J Bacteriol* **135**, 998-1007 (1978).
24 Volle, C. B., Ferguson, M. A., Aidala, K. E., Spain, E. M. & Nunez, M. E. Quantitative changes in the elasticity and adhesive properties of *Escherichia coli* ZK1056 prey cells during predation by *Bdellovibrio bacteriovorus* 109J. *Langmuir : the ACS journal of surfaces and colloids* **24**, 8102-8110, doi:10.1021/la8009354 (2008).
25 Lambert, C., Chang, C. Y., Capeness, M. J. & Sockett, R. E. The first bite-profiling the predatosome in the bacterial pathogen *Bdellovibrio*. *PloS one* **5**, e8599, doi:10.1371/journal.pone.0008599 (2010).
26 Sanders, A. N. & Pavelka, M. S. Phenotypic analysis of *Escherichia coli* mutants lacking L,D-transpeptidases. *Microbiology* **159**, 1842-1852, doi:10.1099/mic.0.069211-0 (2013).
27 Magnet, S. *et al.* Identification of the L,D-transpeptidases responsible for attachment of the Braun lipoprotein to *Escherichia coli* peptidoglycan. *J Bacteriol* **189**, 3927-3931, doi:10.1128/JB.00084-07 (2007).
28 Pilizota, T. & Shaevitz, J. W. Origins of *Escherichia coli* growth rate and cell shape changes at high external osmolality. *Biophys J* **107**, 1962-1969, doi:10.1016/j.bpj.2014.08.025 (2014).
29 Pilizota, T. & Shaevitz, J. W. Plasmolysis and cell shape depend on solute outer-membrane permeability during hyperosmotic shock in E. coli. *Biophys J* **104**, 2733-2742, doi:10.1016/j.bpj.2013.05.011 (2013).
30 Fenton, A. K., Kanna, M., Woods, R. D., Aizawa, S. I. & Sockett, R. E. Shadowing the actions of a predator: backlit fluorescent microscopy reveals synchronous nonbinary septation of predatory *Bdellovibrio* inside prey and exit through discrete bdelloplast pores. *J Bacteriol* **192**, 6329-6335, doi:JB.00914-10 [pii]10.1128/JB.00914-10 (2010).
31 Araki, Y. & Ruby, E. G. A soluble enzyme activity that attaches free diaminopimelic acid to bdelloplast peptidoglycan. *Biochemistry* **27**, 2624-2629 (1988).
32 Shilo, M. Morphological and physiological aspects of the interaction of bdellovibrio with host bacteria. *Current topics in microbiology and immunology* **50**, 174-204 (1969).
33 Iida, Y. *et al.* Roles of multiple flagellins in flagellar formation and flagellar growth post bdelloplast lysis in *Bdellovibrio bacteriovorus*. *J Mol Biol* **394**, 1011-1021, doi:[pii] 10.1016/j.jmb.2009.10.003 (2009).
34 Eksztejn, M. & Varon, M. Elongation and cell division in *Bdellovibrio bacteriovorus*. *Arch Microbiol* **114**, 175-181 (1977).
35 Kuru, E. *et al.* In Situ probing of newly synthesized peptidoglycan in live bacteria with fluorescent D-amino acids. *Angewandte Chemie* **51**, 12519-12523, doi:10.1002/anie.201206749 (2012).
36 Lambert, C. *et al.* Characterizing the flagellar filament and the role of motility in bacterial prey-penetration by *Bdellovibrio bacteriovorus*. *Molecular Microbiology* **60**, 274-286, doi:MMI5081 [pii]10.1111/j.1365-2958.2006.05081.x (2006).
37 Lambert, C. & Sockett, R. Nucleases in *Bdellovibrio bacteriovorus* contribute towards efficient self-biofilm formation and eradication of pre-formed prey biofilms. *FEMS Microbiology Letters* **320**, 109-116, doi:10.1111/1574-6968.12075 (2013).

38 Magnet, S., Dubost, L., Marie, A., Arthur, M. & Gutmann, L. Identification of the L,D-transpeptidases for peptidoglycan cross-linking in *Escherichia coli*. *J Bacteriol* **190**, 4782-4785, doi:10.1128/JB.00025-08 (2008).

39 Baba, T. *et al.* Construction of *Escherichia coli* K-12 in-frame, single-gene knockout mutants: the Keio collection. *Mol Syst Biol* **2**, 2006 0008, doi:10.1038/msb4100050 (2006).

40 Thomason, L. C., Sawitzke, J. A., Li, X., Costantino, N. & Court, D. L. Recombineering: genetic engineering in bacteria using homologous recombination. *Curr Protoc Mol Biol* **14**, 1-39 (2014).

41 Datsenko, K. A. & Wanner, B. L. One-step inactivation of chromosomal genes in *Escherichia coli* K-12 using PCR products. *Proc Natl Acad Sci U S A* **97**, 6640-6645, doi:10.1073/pnas.120163297 (2000).

42 Fenton, A. K., Lambert, C., Wagstaff, P. C. & Sockett, R. E. Manipulating each MreB of *Bdellovibrio bacteriovorus* gives diverse morphological and predatory phenotypes. *J Bacteriol* **192**, 1299-1311, doi:JB.01157-09 [pii]10.1128/JB.01157-09 (2010).

43 Ducret, A., Quardokus, E. M. & Brun, Y. V. MicrobeJ, a tool for high throughput bacterial cell detection and quantitative analysis. *Nat Microbiol* **1**, 16077, doi:10.1038/nmicrobiol.2016.77 (2016).

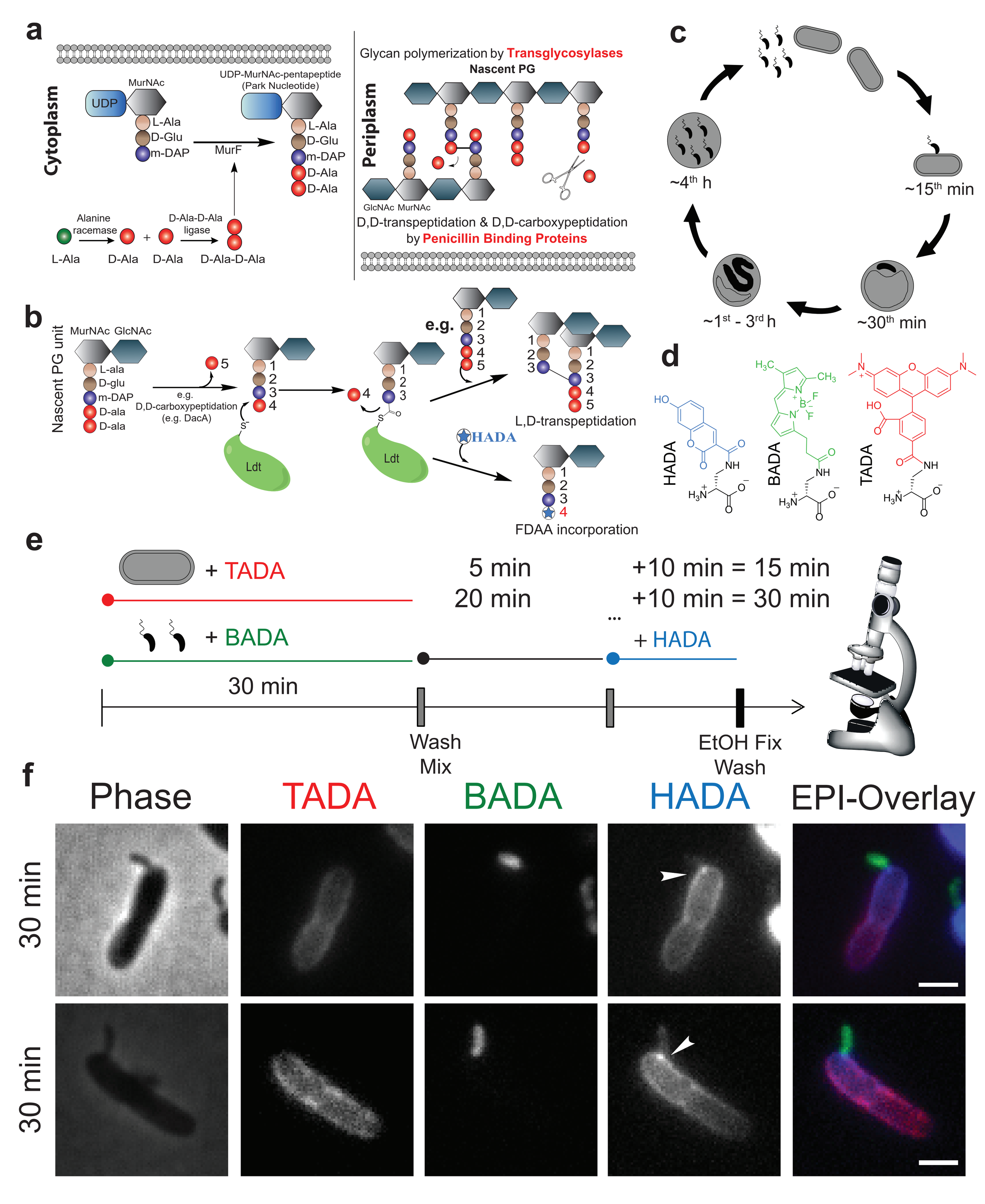
a
Cytoplasm
MurNAc
UDP
L-Ala
D-Glu
m-DAP
UDP-MurNAc-pentapeptide
(Park Nucleotide)
MurF
D-Ala
D-Ala
Alanine
racemase
D-Ala-D-Ala
ligase
L-Ala
D-Ala
D-Ala
D-Ala-D-Ala
Glycan polymerization by Transglycosylases
Nascent PG
Periplasm
GlcNAc MurNAc
D,D-transpeptidation & D,D-carboxypeptidation
by Penicillin Binding Proteins
b
Nascent PG unit
MurNAc GlcNAc
L-ala
D-glu
m-DAP
D-ala
D-ala
e.g.
D,D-carboxypeptidation
(e.g. DacA)
Ldt
Ldt
e.g.
L,D-transpeptidation
HADA
FDAA incorporation
c
~4th h
~15th min
~30th min
~1st - 3rd h
d
HADA
BADA
TADA
e
+ TADA
5 min
20 min
+10 min = 15 min
+10 min = 30 min
...
+ BADA
+ HADA
30 min
Wash
Mix
EtOH Fix
Wash
f
Phase
TADA
BADA
HADA
EPI-Overlay
30 min
30 min

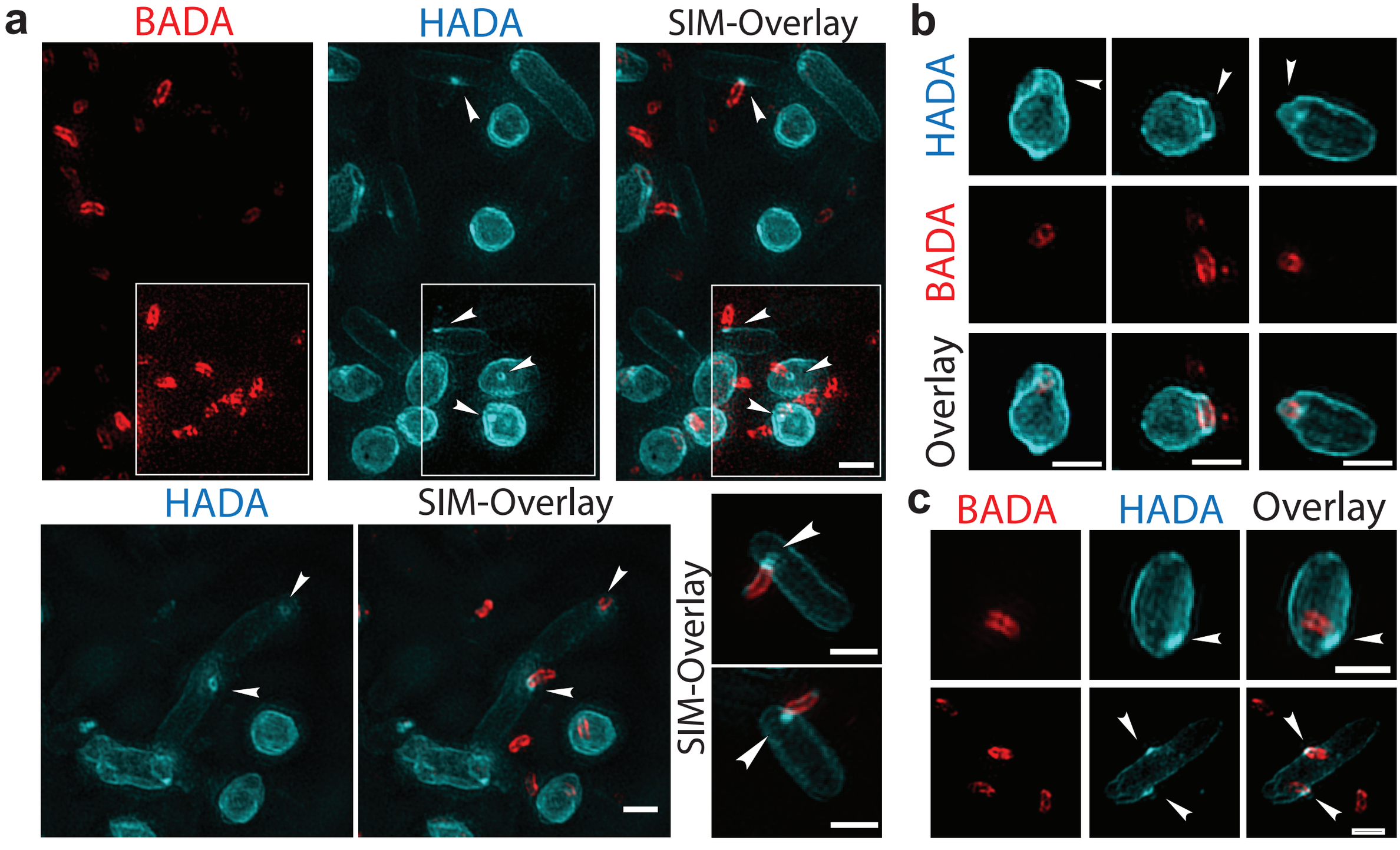
a
BADA
HADA
SIM-Overlay
HADA
SIM-Overlay
SIM-Overlay
b
HADA
BADA
Overlay
c
BADA
HADA
Overlay

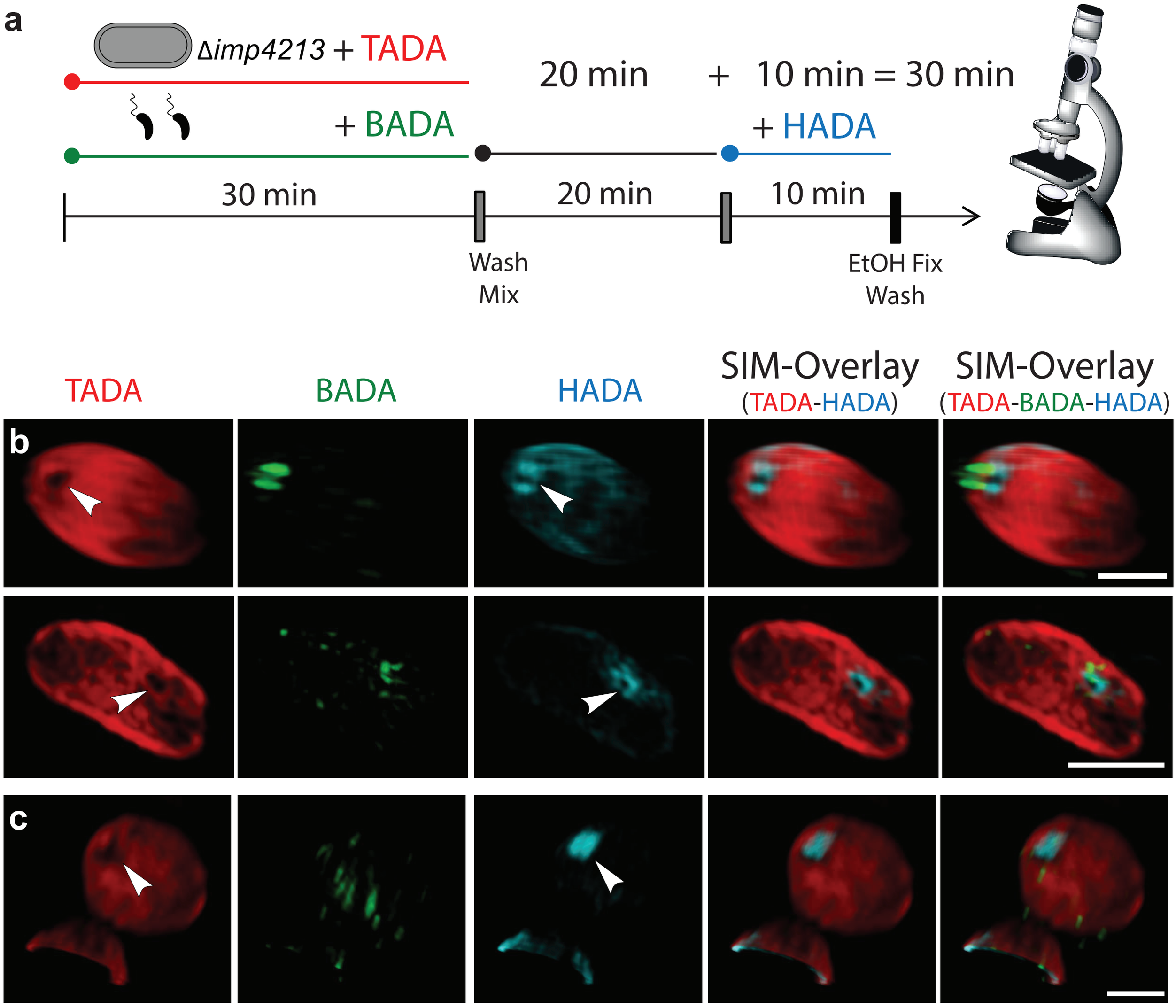
a
Δimp4213 + TADA
+ BADA
20 min + 10 min = 30 min
+ HADA
30 min
20 min
10 min
Wash
Mix
EtOH Fix
Wash
TADA
BADA
HADA
SIM-Overlay
(TADA-HADA)
SIM-Overlay
(TADA-BADA-HADA)
b
c

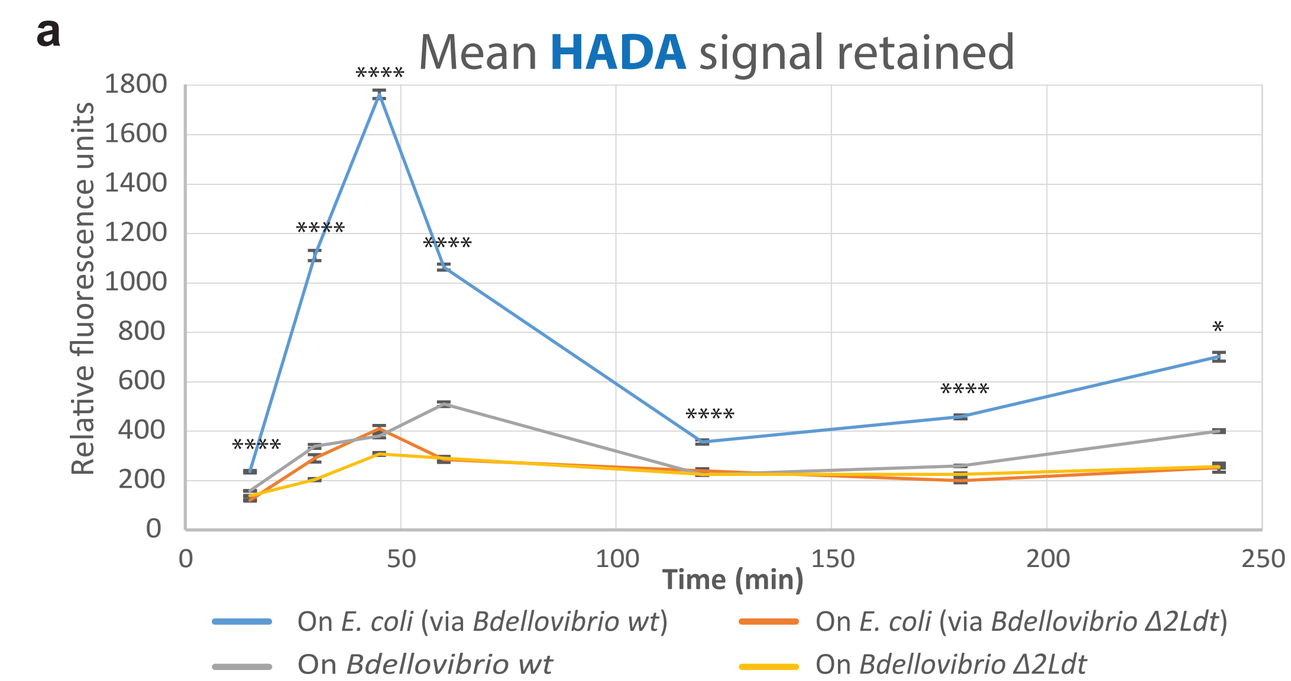
a
Mean HADA signal retained
Relative fluorescence units
1800
1600
1400
1200
1000
800
600
400
200
0
0
50
100
150
200
250
Time (min)
****
*
On E. coli (via Bdellovibrio wt)
On E. coli (via Bdellovibrio Δ2Ldt)
On Bdellovibrio wt
On Bdellovibrio Δ2Ldt

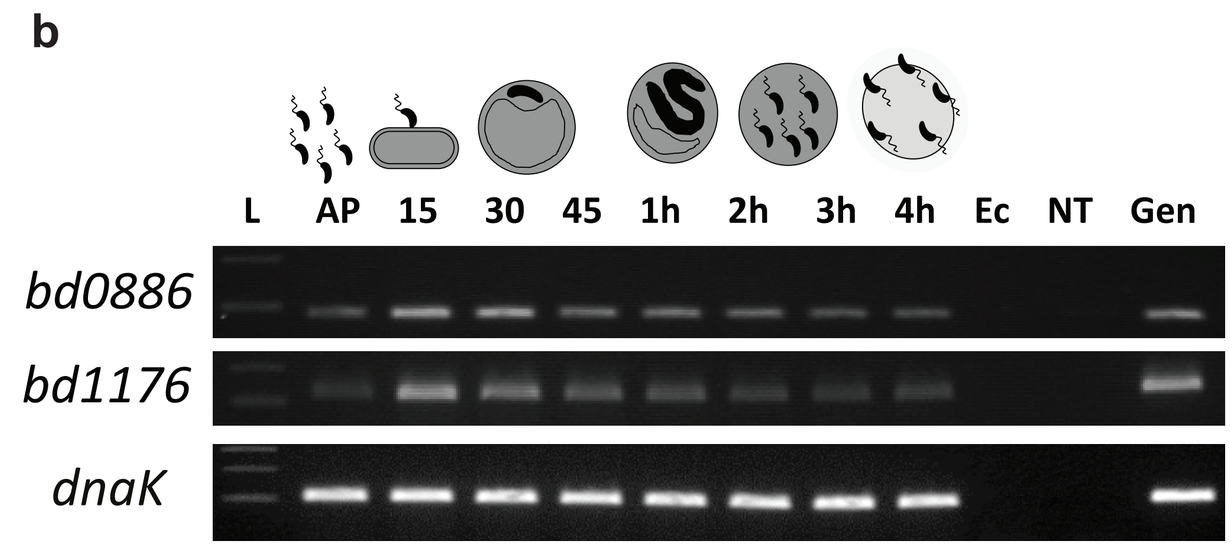
b
L
AP
15
30
45
1h
2h
3h
4h
Ec
NT
Gen
bd0886
bd1176
dnaK

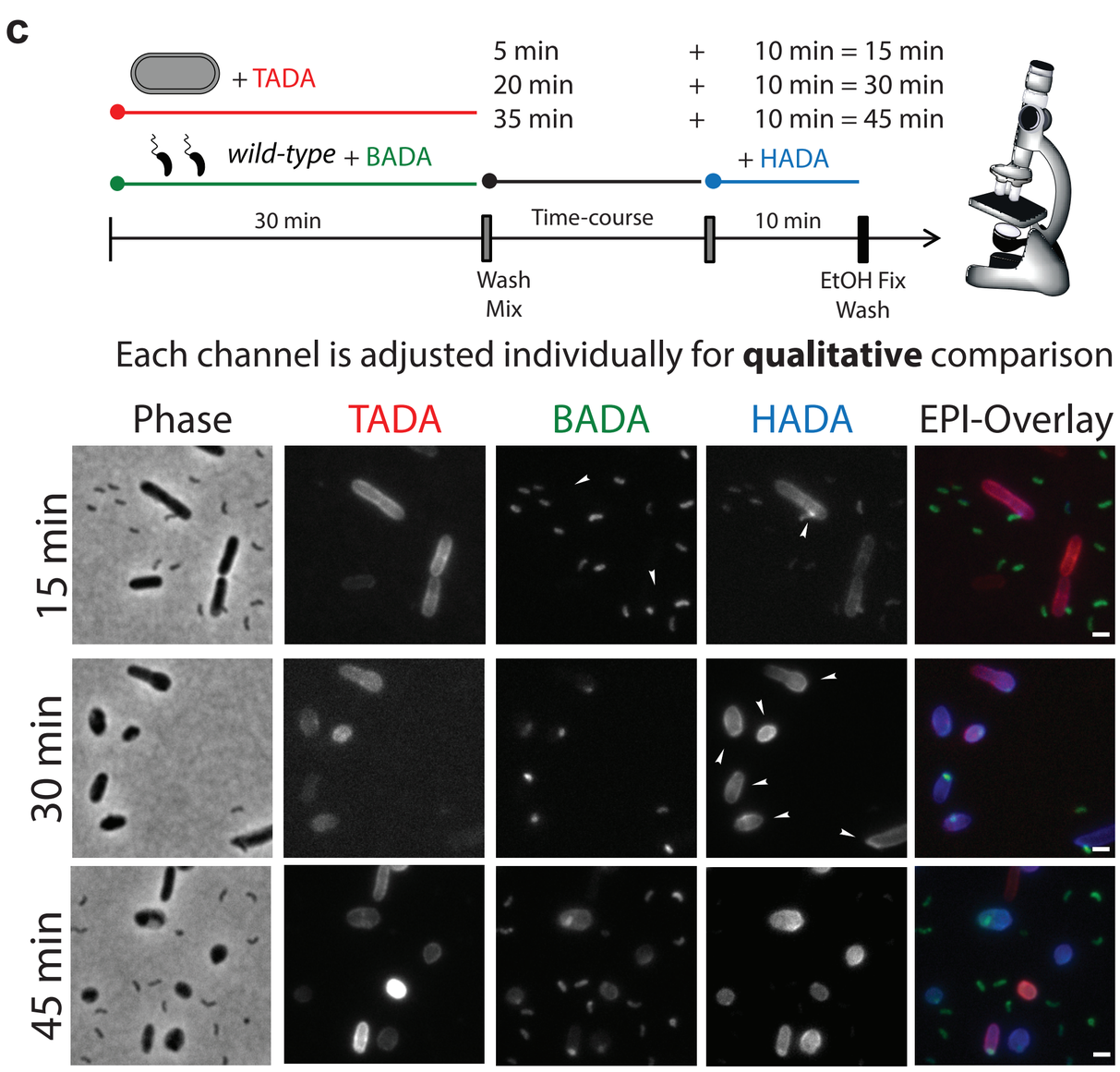
c
+ TADA
wild-type + BADA
5 min + 10 min = 15 min
20 min + 10 min = 30 min
35 min + 10 min = 45 min
+ HADA
30 min
Time-course
10 min
Wash
Mix
EtOH Fix
Wash
Each channel is adjusted individually for qualitative comparison
Phase
TADA
BADA
HADA
EPI-Overlay
15 min
30 min
45 min

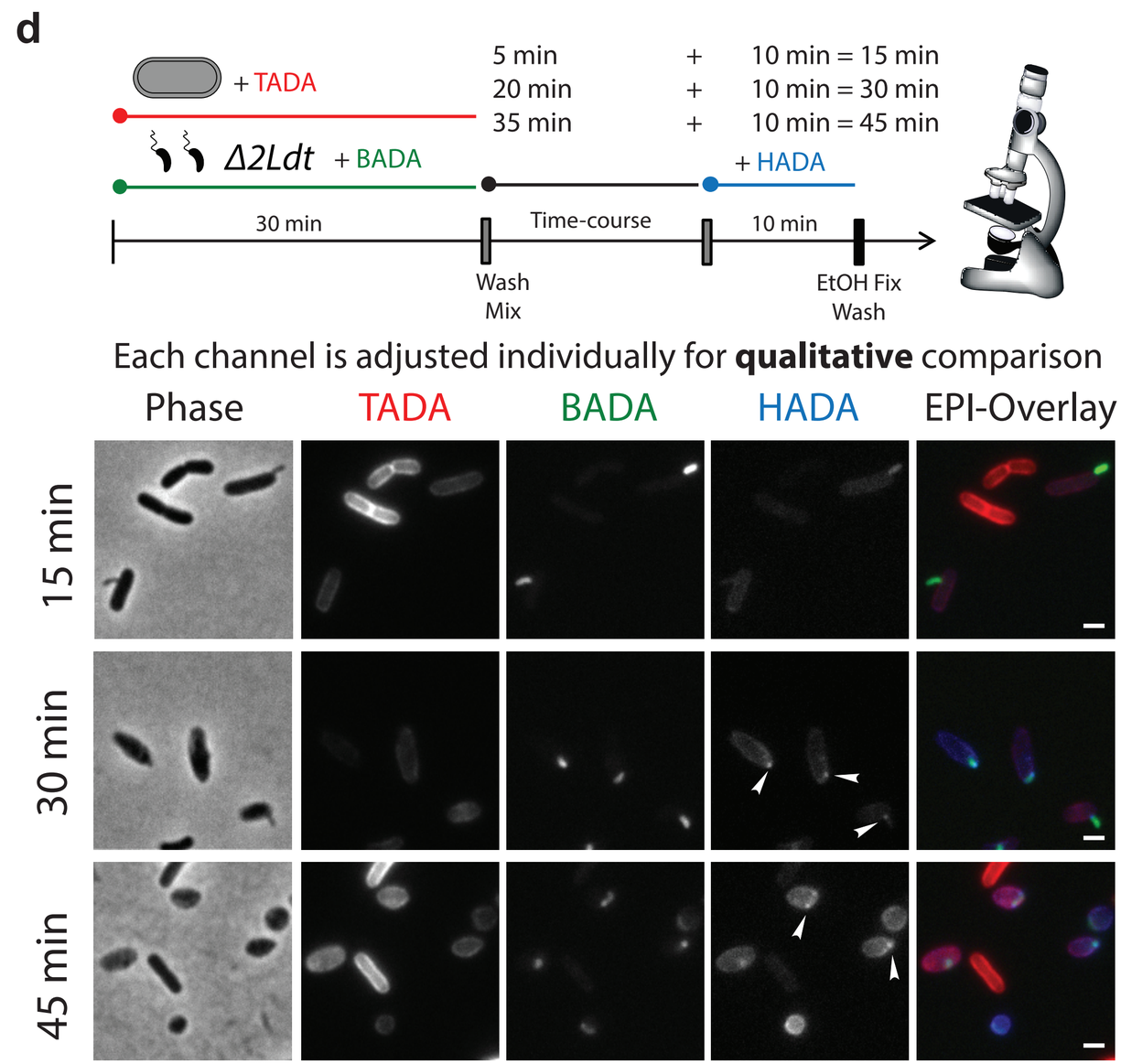
d
+ TADA
Δ2Ldt + BADA
5 min + 10 min = 15 min
20 min + 10 min = 30 min
35 min + 10 min = 45 min
+ HADA
30 min
Time-course
10 min
Wash
Mix
EtOH Fix
Wash
Each channel is adjusted individually for qualitative comparison
Phase
TADA
BADA
HADA
EPI-Overlay
15 min
30 min
45 min

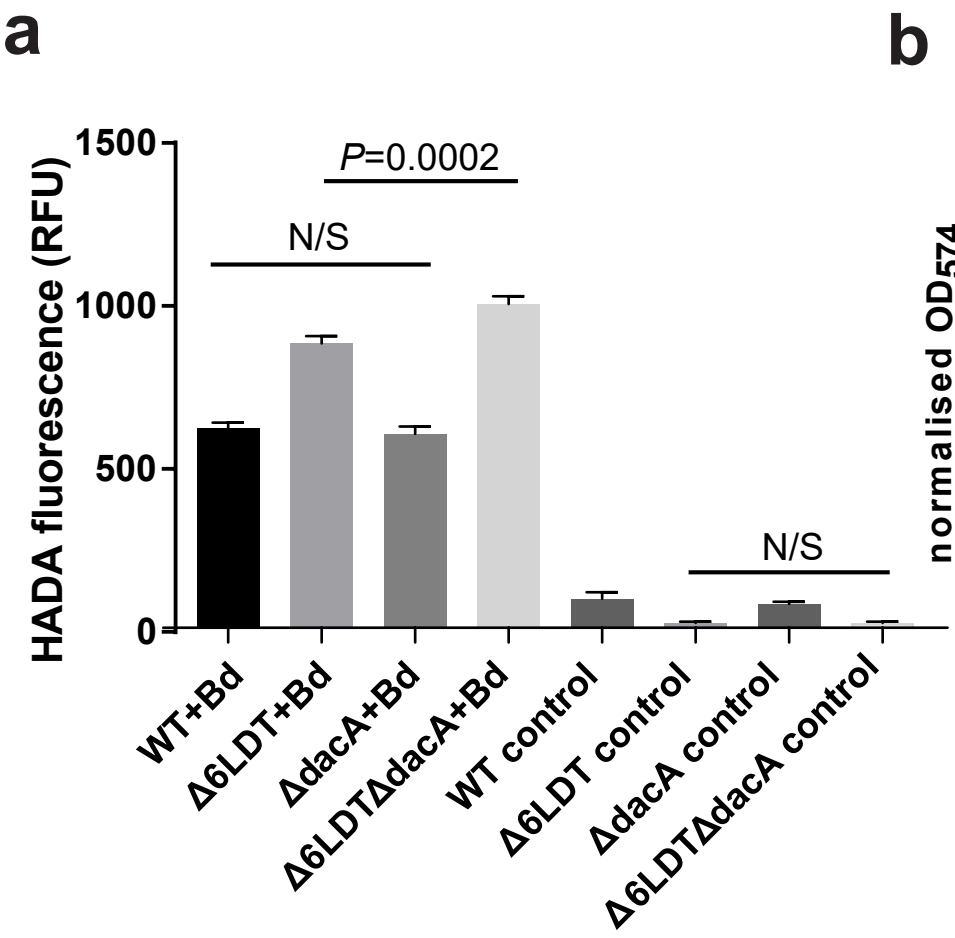
a
HADA fluorescence (RFU)
1500
1000
500
0
P=0.0002
N/S
N/S
WT+Bd
Δ6LDT+Bd
ΔdacA+Bd
Δ6LDTΔdacA+Bd
WT control
Δ6LDT control
ΔdacA control
Δ6LDTΔdacA control

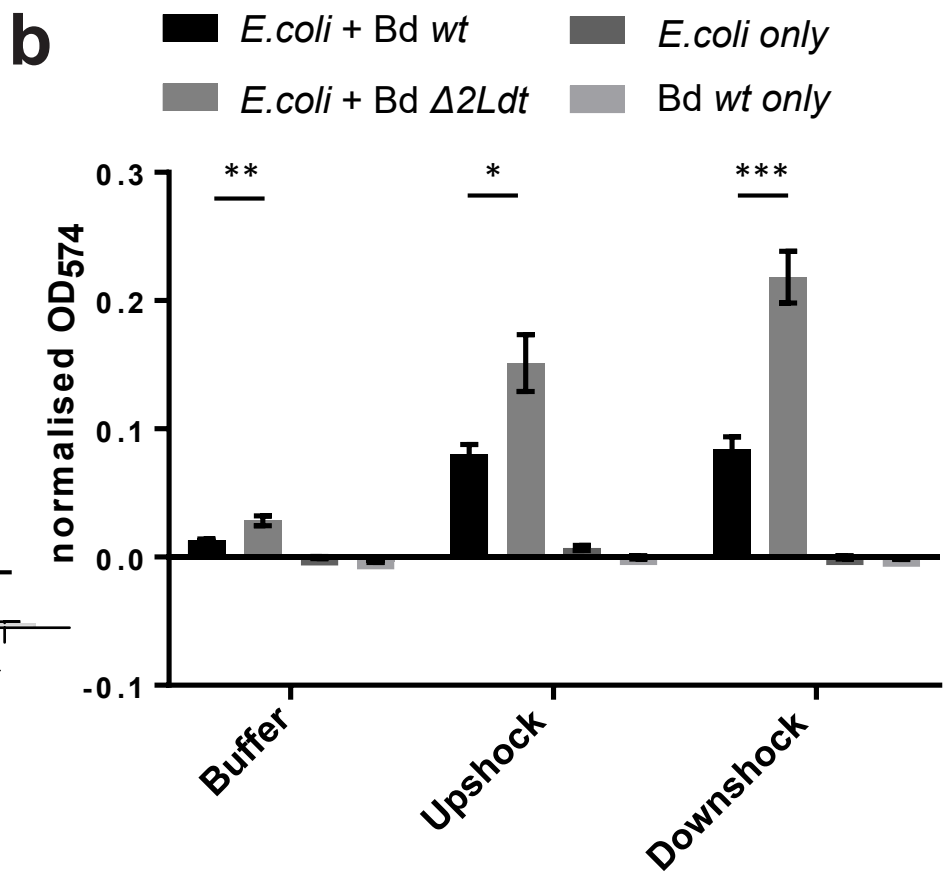
b
E.coli + Bd wt
E.coli + Bd Δ2Ldt
E.coli only
Bd wt only
normalised OD574
0.3
0.2
0.1
0.0
-0.1
**
*
***
Buffer
Upshock
Downshock

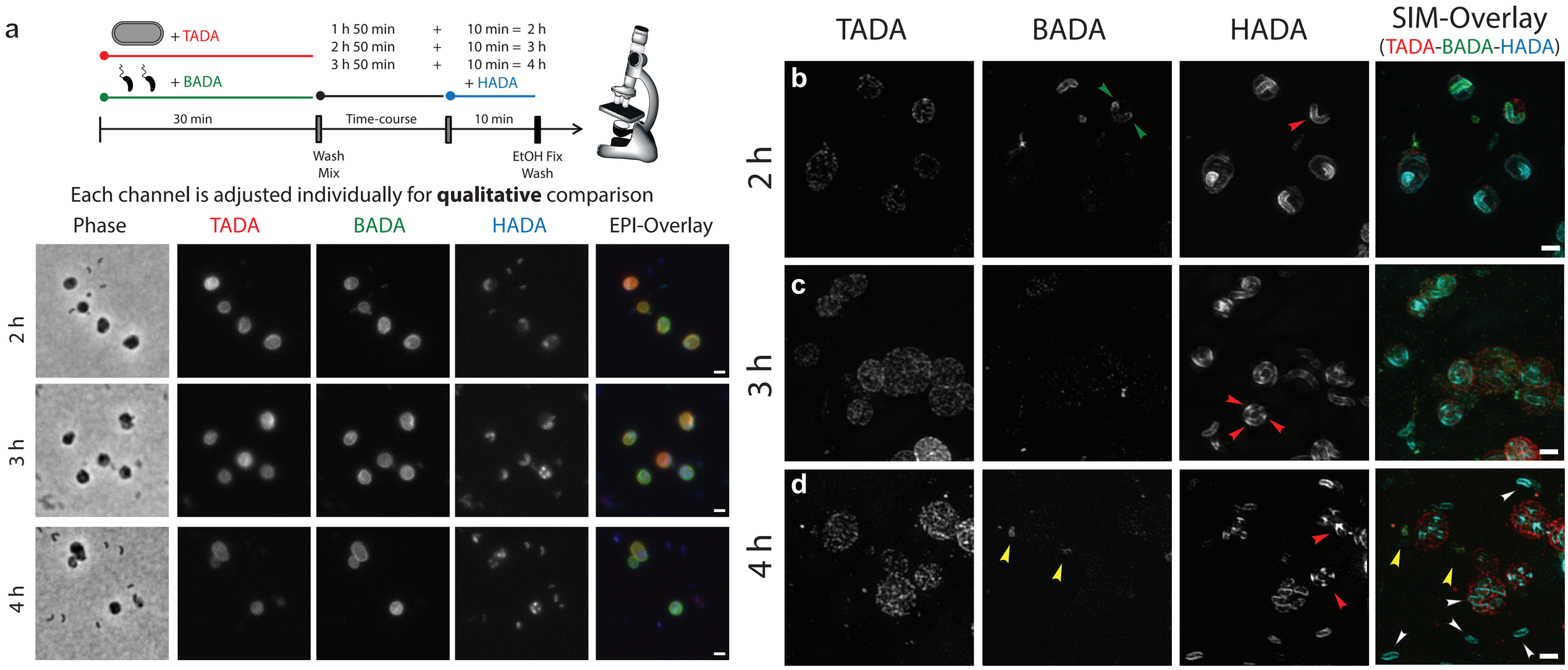
a
+ TADA
+ BADA
1 h 50 min + 10 min = 2 h
2 h 50 min + 10 min = 3 h
3 h 50 min + 10 min = 4 h
+ HADA
30 min
Time-course
10 min
Wash
Mix
EtOH Fix
Wash
Each channel is adjusted individually for **qualitative** comparison
Phase
TADA
BADA
HADA
EPI-Overlay
2 h
3 h
4 h
TADA
BADA
HADA
SIM-Overlay
(TADA-BADA-HADA)
b
c
d
2 h
3 h
4 h

**Supplementary information for "Bi-cellular wall modifications during *Bdellovibrio bacteriovorus* predation include pore-formation and L,D-transpeptidase mediated prey strengthening"**

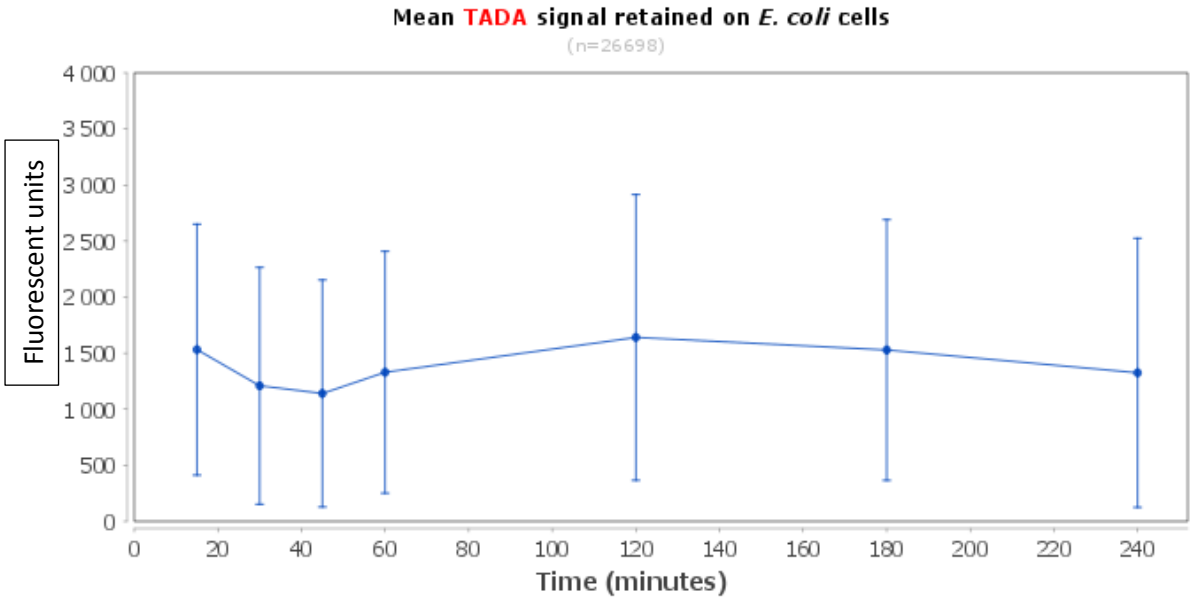


**Supplementary Figure 1** Plot of mean TADA fluorescent signal of cells against time throughout the predation cycle. Measurements are total mean TADA fluorescent signal from free uninvaded *E. coli* prey cells or invaded prey bdelloplast. Time is in minutes post-mixing of predator and prey and fluorescence is in relative fluorescent units measured by MicrobeJ (see methods). n= 26,698. Details of numbers of cells analysed at each time point are elaborated below. Error bars are one standard deviation.

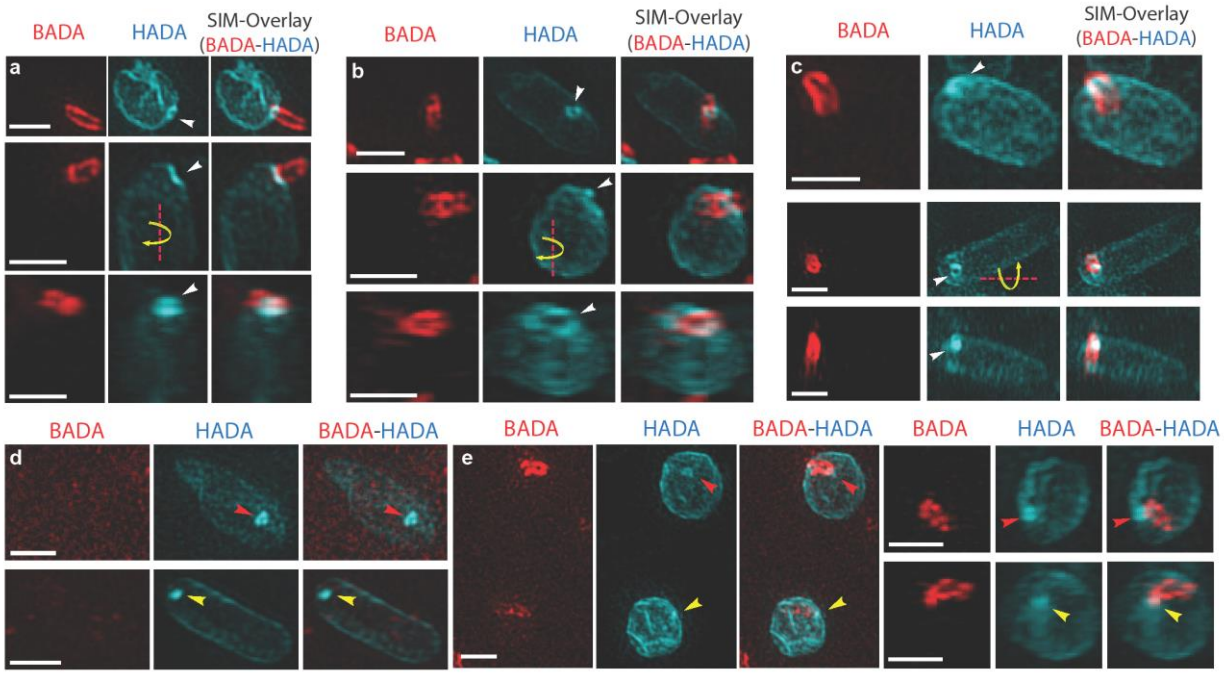


**Supplementary Figure 2** 3D-SIM images of early predation by *B. bacteriovorus* (pre-labelled with BADA, false-coloured red) on prey *E. coli* cells after a pulse labelling for 10 minutes with HADA (false-coloured cyan) to show early modification of cell walls. **a-** Examples of *B. bacteriovorus* cells in the very earliest stages of prey entry through a pore of HADA modification. Here, only the very front of the predator has penetrated the prey PG. **b-** Examples with the *B. bacteriovorus* cell half way through the HADA labelled pore. **c-** Examples of *B. bacteriovorus* cells mostly through the HADA labelled pore; only the very rear of the predator cell has not passed through the prey PG. The lowest panels in **a-c** show the same cells as the middle panels from a different angle. Yellow arrows indicate the direction of rotation around the axis represented by the red dashed line to move from the angle shown in the middle panel to the angle shown in the lower panel. **d-** Examples of HADA modification on the prey cell wall in the absence of a *B. bacteriovorus* cell. Either a ring (red arrowheads) or disc (yellow arrowheads) of HADA modification can be seen. The lookup tables for the BADA channel have been adjusted until the background signal is very high to show that there is not any *B. bacteriovorus* cells with low level labelling attached. Instead, these seem to be examples where the *B. bacteriovorus* cell has become detached soon after modifying the prey

PG, likely as a result of the centrifugation and washing steps of the labelling procedure. This shows that the HADA rings of modification are indeed on the prey PG rather than waves of modification moving along the entering *B. bacteriovorus* cell. **e-** Examples of the two forms of seal highlighted by HADA labelling. The internalised *B. bacteriovorus* cell has a contact point with the prey PG where a small ring of HADA is visible (red arrowheads, top cells) or a filled disc of HADA labelling (yellow arrowheads, lower cells). Scale bars are 1µm. Data are representative of two independent repeats.

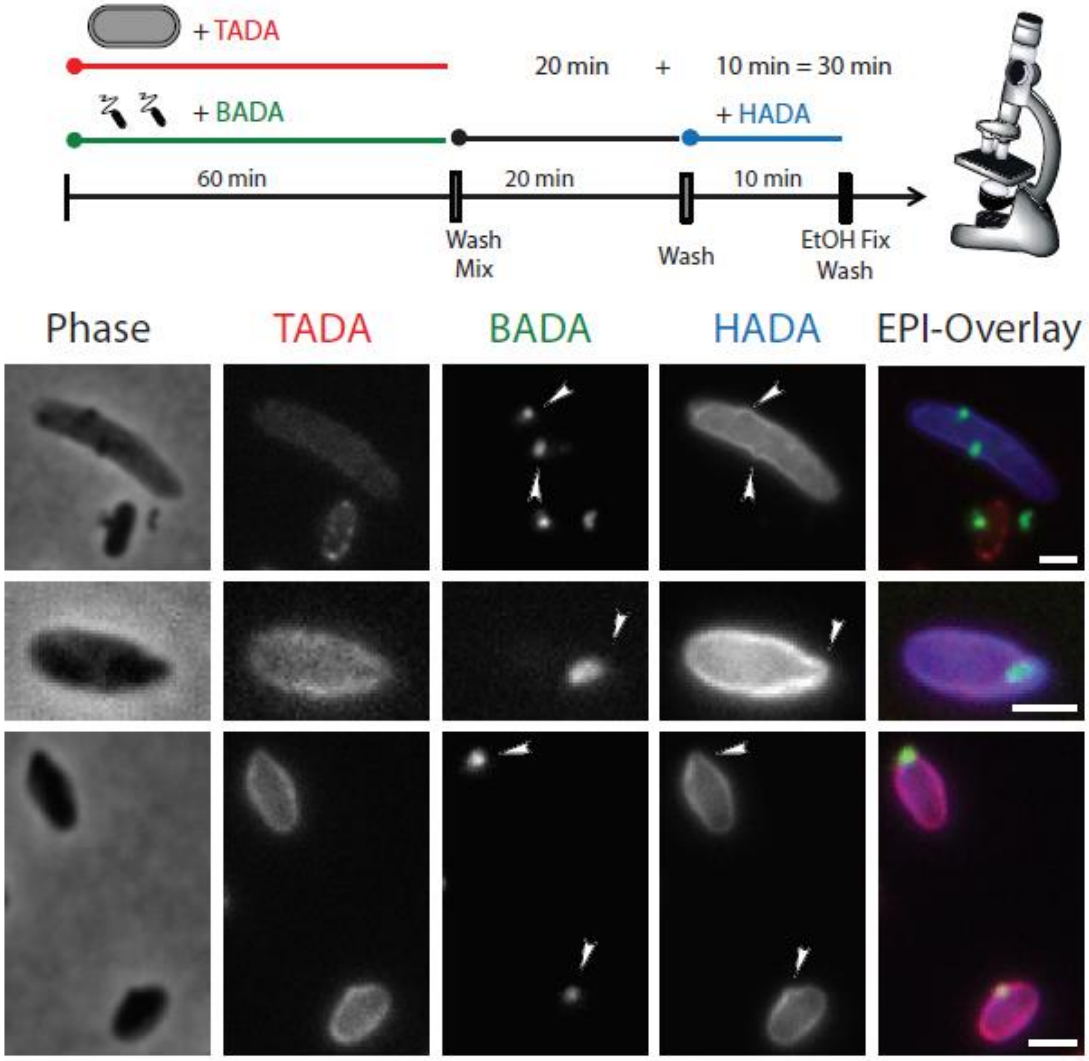


**Supplementary Figure 3-** Phase contrast and epi-fluorescent microscopy images of the early stages of *Bdellovibrio* predation. The *Bdellovibrio* were pre-labelled with BADA and are false-coloured in green, the *E. coli* prey cells were pre-labelled with TADA and are false-coloured in red. The cells were pulse-labelled for 10 minutes before each acquisition time point with HADA, which is false-coloured in blue. Each channel is displayed independently in white and with all 3 fluorescence channels merged in EPI-overlay. The prey cell wall bulges around the invading *Bdellovibrio* cell to allow the predator entry to the confined space of the periplasm (arrowheads). Data are representative of five independent repeats. Scale bars are 1 µm.

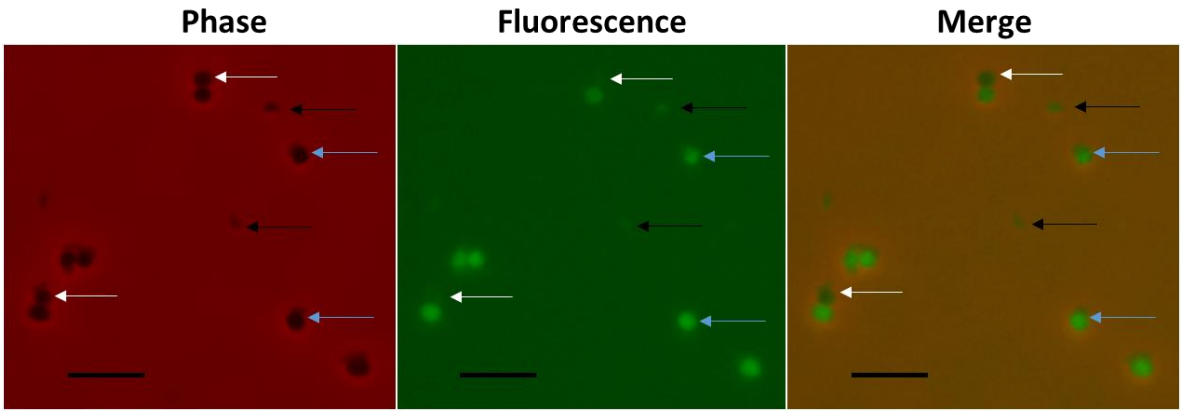


**Supplementary Figure 4** Epifluorescent images of *E. coli* invaded by *B. bacteriovorus* HD100 with C-terminally mCherry tagged Bd1176 protein at 45 minutes post-infection. Fluorescence was acquired with a two second exposure and maximum sensitivity gain. mCherry fluorescence has been false-coloured in green. The fluorescent tag was localised to the bdelloplasts (blue arrows) indicating that the protein was exported into the bdelloplast periplasm and/or cytoplasm, consistent with it acting on the prey cell wall. Some bdelloplasts showed low levels of fluorescence (white arrows) as they were likely very recently formed bdelloplasts in this semi-synchronous infection and this is in agreement with the variable levels of HADA incorporation effected by this protein and Bd0886. The *Bdellovibrio* cells themselves (black arrows) also showed a low level of fluorescence suggesting that the protein is either pre-produced in an inactive form, or that the *Bdellovibrio* have a mechanism to control its activity within the *Bdellovibrio* periplasm, such as an associated immunity protein. An immunity protein has recently been described which protects *B. bacteriovorus* from its own predatory DacB enzymes which round up the bdelloplast[1] Scale bars are 5 µm. Data are representative of three independent repeats.

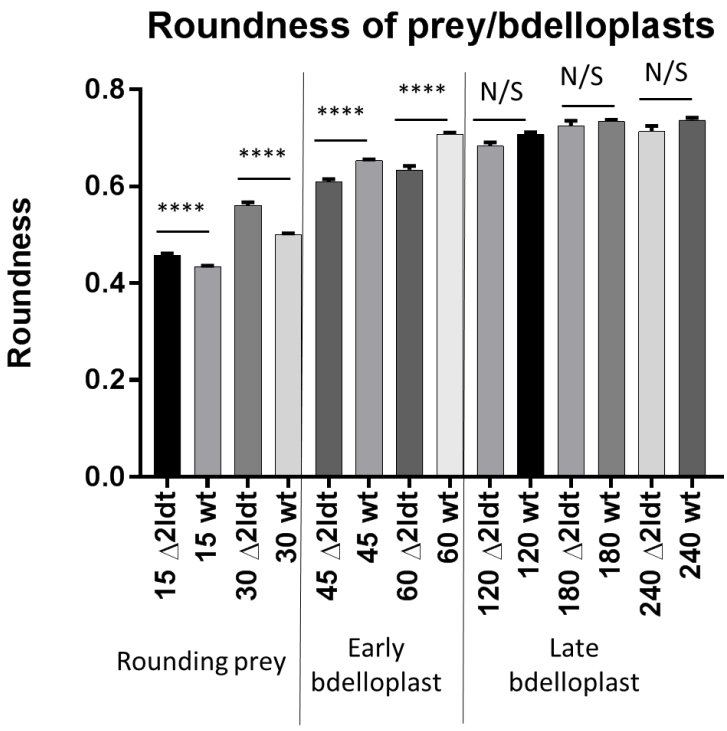


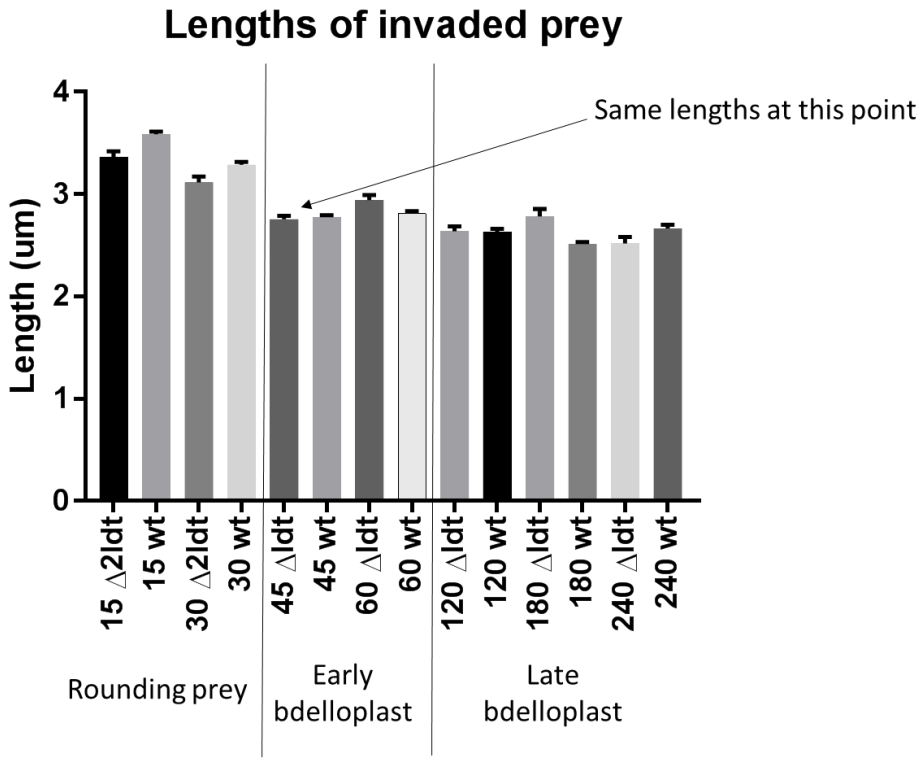


**Supplementary Figure 5**- Morphology of prey and bdelloplasts formed by predation by *Δ2ldt* mutants compared to wild type. **a-** roundness **b-** lengths as measured by the MicrobeJ

plugin for ImageJ. (Prey gradually transform and shorten, from rod shaped to rounded, by the action of predators and eventually reach maximum morphological modification by predators which are now internal). At the 15 and 30 minute timepoints, prey cells mixed with wild-type predator are less round and longer than the prey cells mixed with *Δ2ldt* predators. This is likely the result of slight asynchrony of the predatory process in these experiments with the *Δ2ldt* mutants preying slightly faster than the wild-type. At the 45 minute timepoint, the lengths of the prey of the wild type and *Δ2ldt* predator are equal suggesting that at this point, virtually all of the prey have formed bdelloplasts. At this timepoint and at 60 minutes, the bdelloplasts formed by the *Δ2ldt* mutant are significantly less round than those formed by the wild-type. We hypothesise that this may be the result of the wild-type predator Ldt action strengthening the bdelloplast wall and the weaker bdelloplast wall formed by the *Δ2ldt* mutant predator being more warped by the invading predator cells. This difference was not observed to be significant at later timepoints; this could be due to predator degradation of the prey contents relieving outward osmotic pressure within the bdelloplast. **** $p<0.0001$ by the Mann-Whitney test, between prey mixed with *Δ2ldt* and wild-type predators. Roundness is measured in arbitrary units defined by the MicrobeJ plugin as $4 \times [Area] / (\pi \times [Major\ axis]^2)$. Data are from two independent repeats for the *Δ2ldt* mutant and five independent repeats for the wild-type. Error bars are SEM.

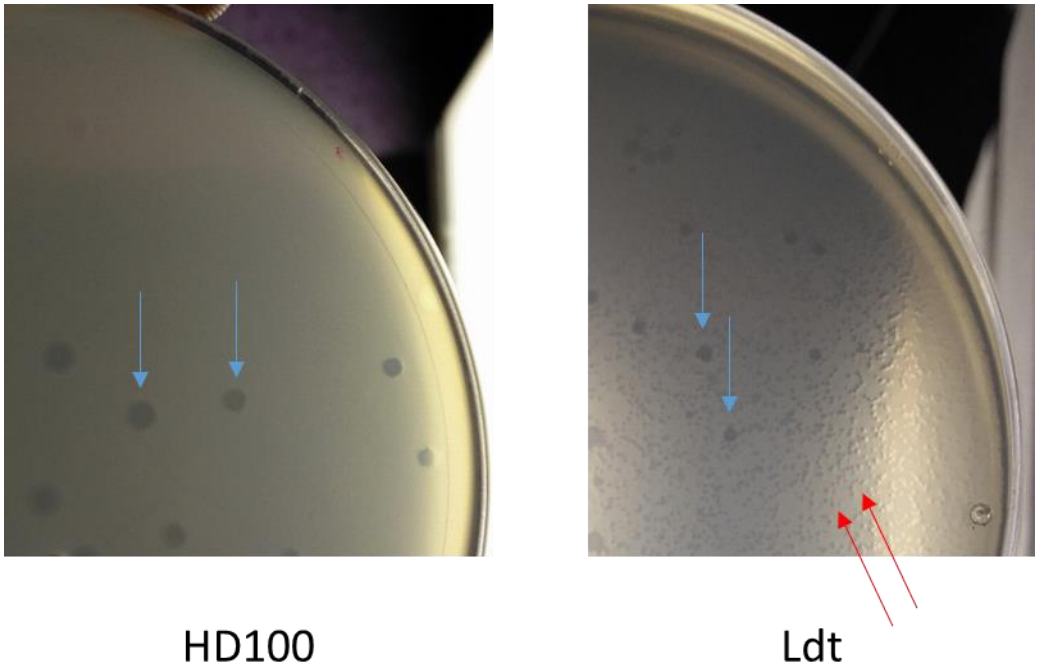


**Supplementary Figure 6**- Double-layer overlay agar petri dishes demonstrating plaque formation by wild-type (HD100) and mutant *Δ2ldt Bdellovibrio.* YPSC media was used with 1% agar in the bottom layer and 0.6% agar in the top layer, which is supplemented with 100 µl of stationary phase prey *E. coli* to form a lawn and 100 µl of $10^{-4}$ to $10^{-7}$ dilutions of concentrated *Bdellovibrio* samples (see methods) to form plaques. Plaques form as regions of clearing in the prey lawn, becoming 4-8 mm in diameter in the wild-type and a minority of plaques formed by the *Δ2ldt* mutant after 5-8 days incubation at 29°C (blue arrows). The majority of plaques formed by the *Δ2ldt* mutant only grow to 1-3 mm in this incubation time (red arrows). Images are representative of plates from 7 independent repeats.

A

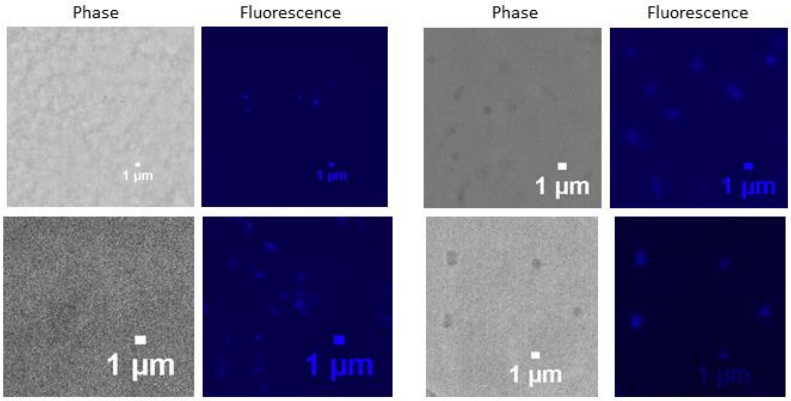
*Bdellovibrio* sacculi
*E. coli* sacculi
Phase
Fluorescence
Phase
Fluorescence
Br-HADA labelled
HADA labelled
1 µm

B

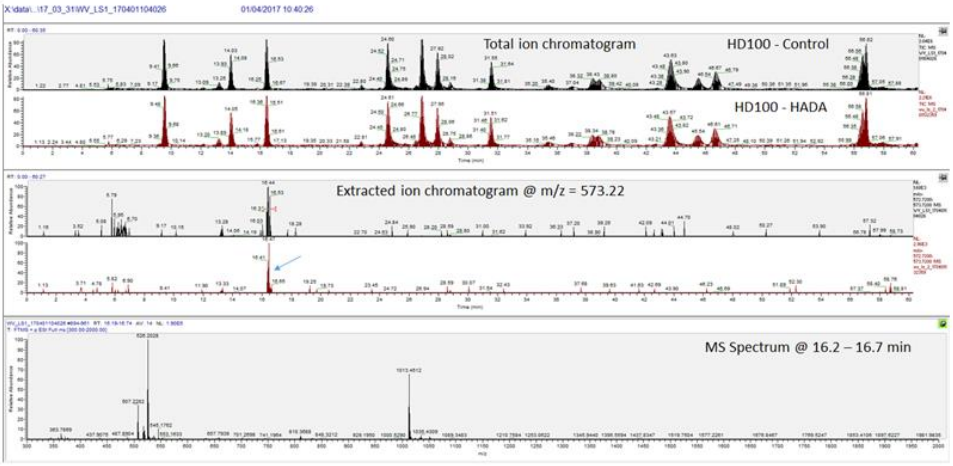
Total ion chromatogram
HD100 - Control
HD100 - HADA
Extracted ion chromatogram @ m/z = 573.22
MS Spectrum @ 16.2 – 16.7 min

C

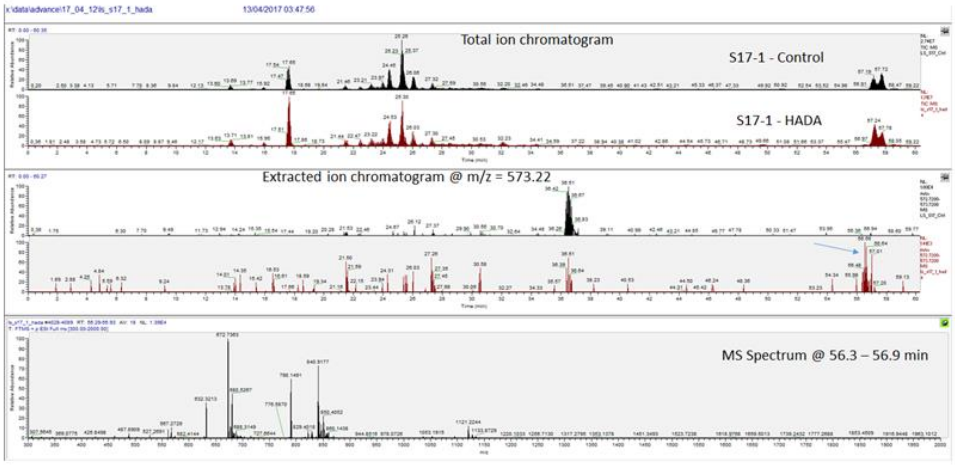
Total ion chromatogram
S17-1 - Control
S17-1 - HADA
Extracted ion chromatogram @ m/z = 573.22
MS Spectrum @ 56.3 – 56.9 min

1020

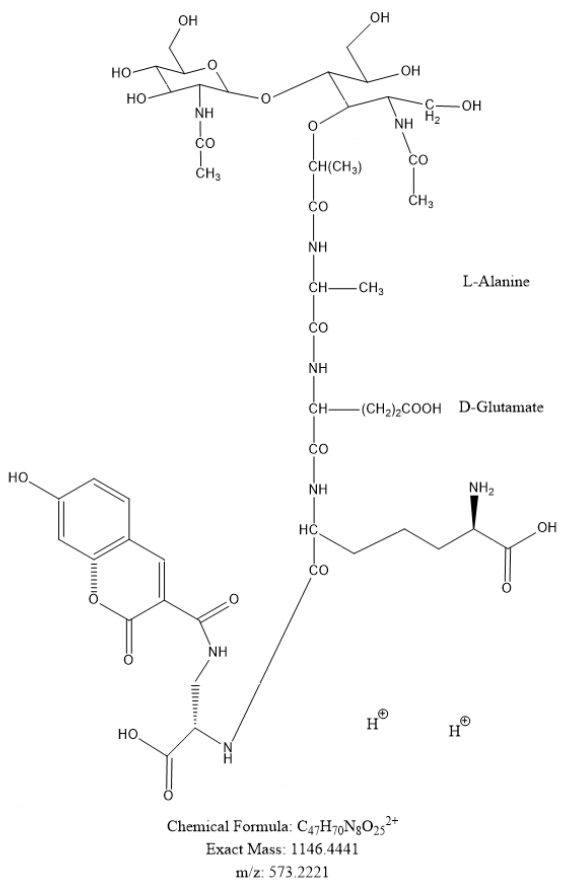


**Supplementary Figure 7-** Analysis of PG sacculi from *Bdellovibrio* and *E. coli* cells labelled *in vivo* with FDAAs. (A) Live cells of *Bdellovibrio* and *E. coli* were labelled with Br-HADA or HADA. PG sacculi were isolated and visualized by phase contrast and epifluorescence microscopy. Images are representative of one attempt of labelling with each FDAA. Sacculi from *E. coli* (B) or *Bdellovibrio* (C) were digested with cellosyl and the resulting muropeptides were reduced and analysed by LC-MS/MS. The top panels show total ion chromatogram traces for both the unlabelled control (black) and HADA-labelled (red) samples respectively. The middle panels show plots of extracted ion chromatograms (selected m/z = 573.22 ) for the same samples. The mass filter was set at m/z = 573.22 to correspond with the $2H^+$ charged ion of the expected major HADA-labelled muropeptide [shown in (D)]. The bottom panels in (B) and (C) show the mass spectra observed at the retention times (blue arrow, middle panel) where the 573.22 ion species was most intense in the corresponding HADA-labelled samples (between 16.2 and 16.7 min and 53.6 and 53.9 min respectively). In neither

instance was sufficient ion signal present to permit positive confirmation of the desired HADA-labelled muropeptide.

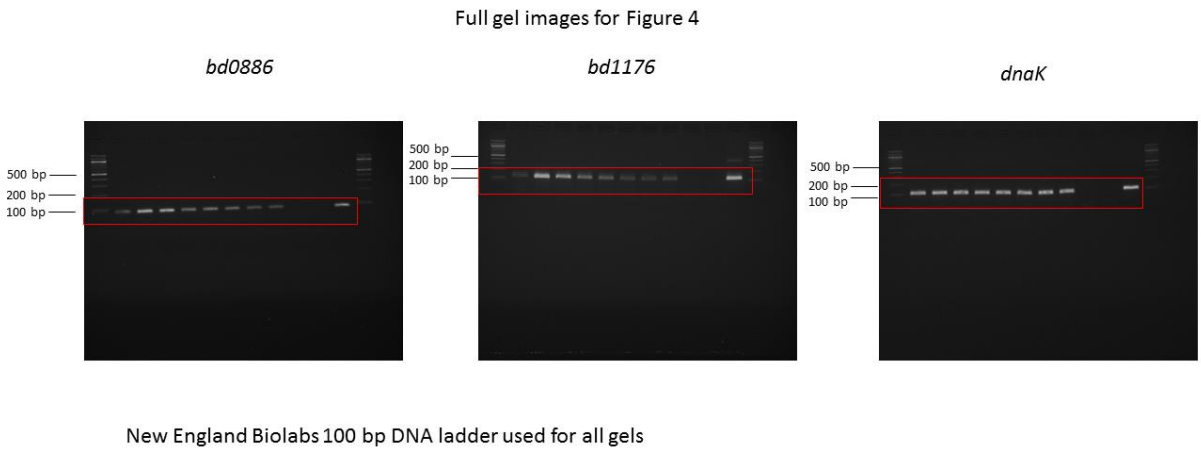


**Supplementary Figure 8-** Full, uncropped images of the gels used for Figure 4 with the cropped regions highlighted. Primers designed to anneal specifically to the gene labelled above each gel were used for RT-PCR.

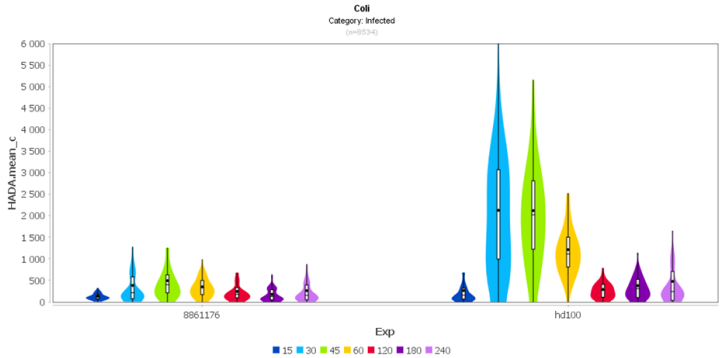


Plot to show distribution of data for figure 4a

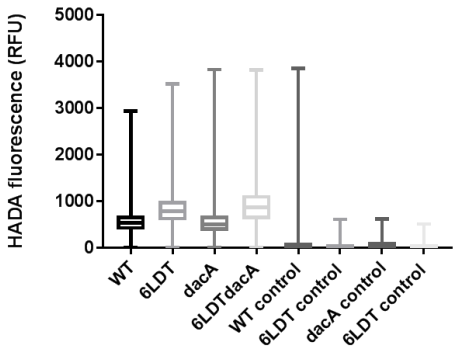


Plot to show data distribution in Figure 5a

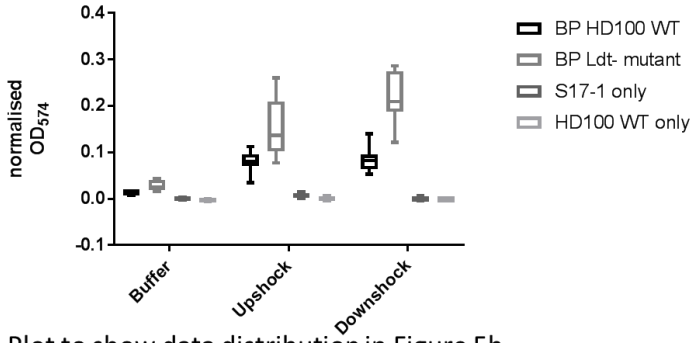


Plot to show data distribution in Figure 5b

1042

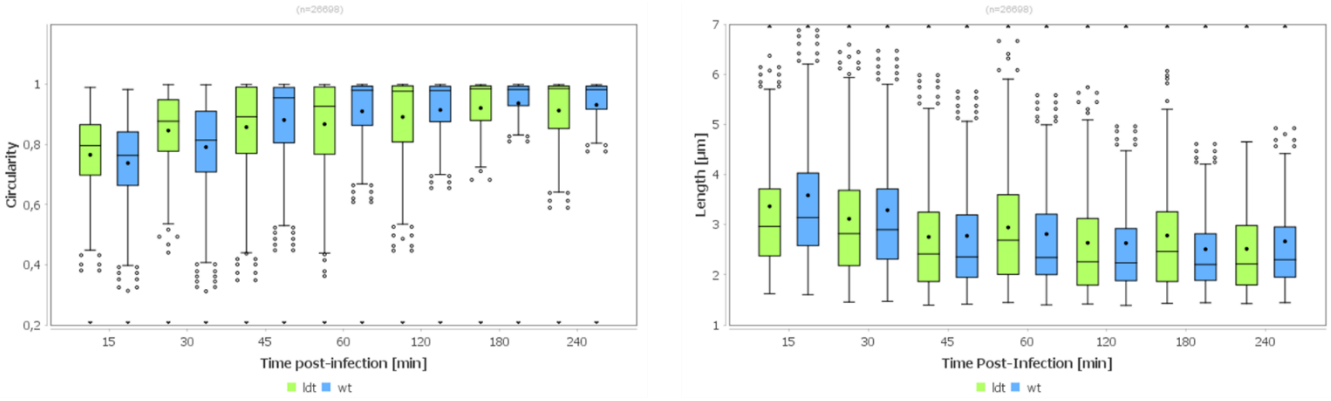


Plots to show data distribution in Supplementary figure 5

1043

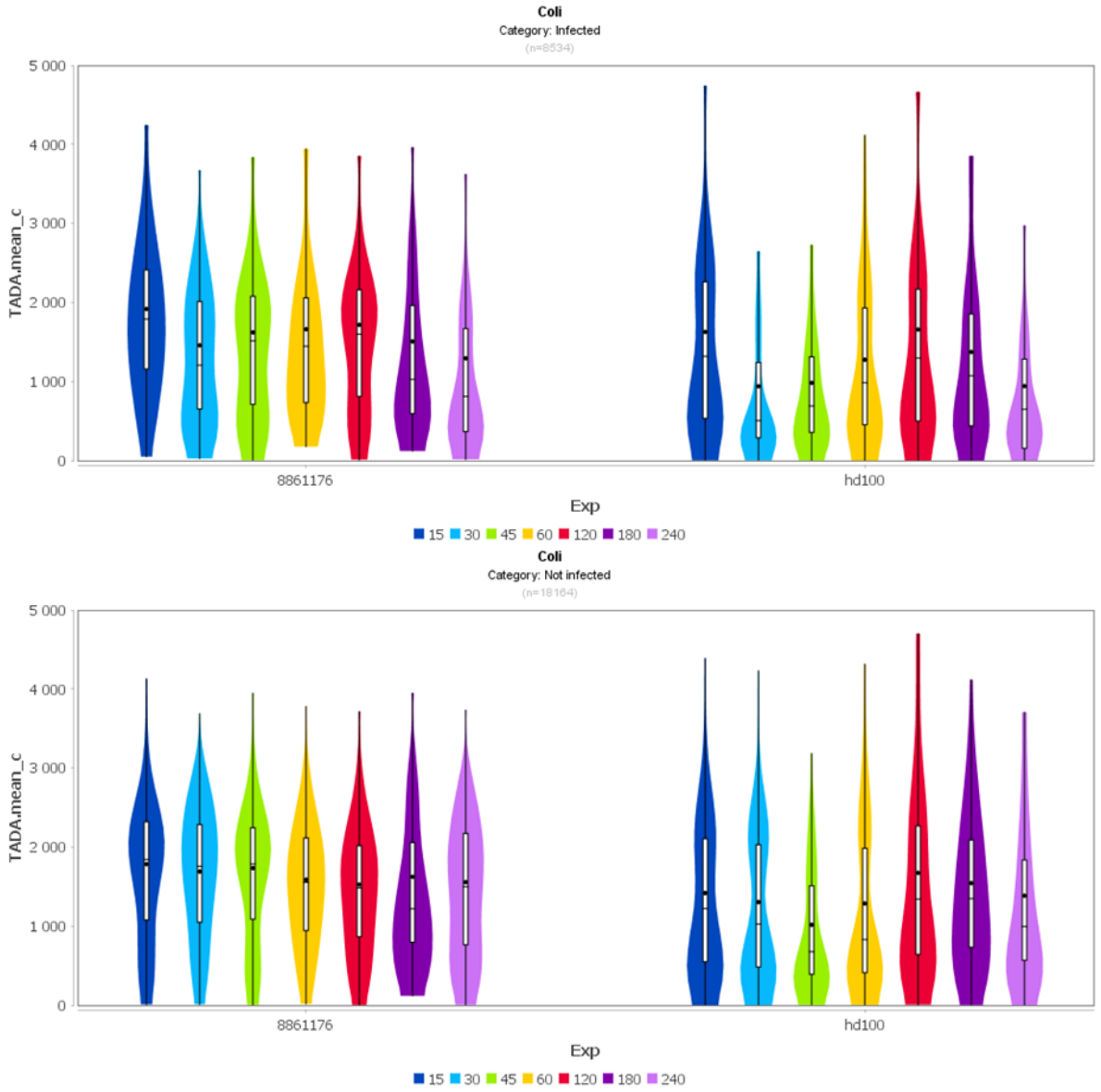


Plot to show data distribution in Supplementary Figure 1

**Supplementary Figure 9-** Plots to show data distribution.

| **Mutant prey experiments** | **WT keio** | **6LDT** | **dacA** | **6LDTdacA** | **WT control** | **6LDT control** | **dacA control** | **6LDTdacA control** |
|---|---|---|---|---|---|---|---|---|
| n1 | 208 | 220 | 239 | 338 | 111 | 105 | 40 | 92 |
| n2 | 106 | 76 | 38 | 30 | 204 | 77 | 46 | 57 |
| n3 | 344 | 260 | 45 | 247 | - | - | - | - |
| totals | 658 | 556 | 322 | 615 | 315 | 182 | 86 | 149 |
| **Timepoint (minutes) S17-1 experiments** | | **15** | **30** | **45** | **60** | **120** | **180** | **240** |
| Prey cells/bdelloplasts | HD100 | 395 | 1210 | 1879 | 1528 | 141 | 203 | 190 |
| | *Δ2ldt* | 159 | 226 | 510 | 237 | 187 | 89 | 85 |
| *Bdellovibrio* cells | HD100 | 4381 | 2388 | 2034 | 3721 | 1348 | 3379 | 4966 |
| | *Δ2ldt* | 1511 | 2286 | 2555 | 933 | 2411 | 1062 | 1912 |
| **Timepoint (minutes) morphology experiments** | | **15** | **30** | **45** | **60** | **120** | **180** | **240** |
| Prey cells/bdelloplasts | HD100 | 3692 | 3632 | 5511 | 3639 | 1994 | 1993 | 1110 |
| | *Δ2ldt* | 1063 | 642 | 1387 | 627 | 818 | 321 | 269 |

**Supplementary Table 1- Numbers of cells analysed for each experiment.** Numbers of cells analysed using the MicrobeJ plugin for ImageJ (FIJI release) for the different experiments. For the FDAA labelling of mutant prey experiment: WT- *E. coli* BW25113 wild-type strain YB7421, 6LDT- *E. coli* BW25113 Δ6LDT deficient in all 6 L,D transpeptidases, dacA- *E. coli* BW25113 strain YB7423 deficient in DacA, 6LDTdacA- *E. coli* BW25113 strain YB7439 deficient in all 6 L,D transpeptidases and DacA. Three independent repeats were carried out with *Bdellovibrio* and 2 independent repeats were carried out in control experiments without *Bdellovibrio* added. For the FDAA labelling of predation on *E. coli* S17-1 experiments and for the prey cell/bdelloplast morphology experiments, five independent repeats were carried out for the HD100 wild-type experiments and two independent repeats were carried out for the *Δ2ldt* mutant experiments. RT-PCR experiments were carried out on RNA isolated from two independent repeats, with the expression patterns for test and control genes in agreement in both experiments.

| | instances | % of instances | Average long axis diameter in nm | Std-dev | instances | % of instances | Average long axis diameter in nm | Std-dev |
|---|---|---|---|---|---|---|---|---|
| Timepoint | **15 min** | | | | **30 min** | | | |
| Number of HADA-bright prey cells investigated | 202 | - | - | - | 229 | - | - | - |
| # of invaded prey (half-entered counted as 0.5) | 147 | 72.8 | - | - | 180 | 78.6 | - | - |
| # of predator outside AND touching (half-entered counted as 0.5) | 47.5 | 23.5 | - | - | 44.5 | 19.4 | - | - |
| # of prey with **multiple** predators inside | 13 | 6.4 | - | - | 19 | 8.3 | - | - |
| Predation related cellular features in HADA-bright prey cells investigated | | | | | | | | |
| # of bdelloplasts | 158 | 78.2 | - | - | 201 | 87.8 | - | - |
| # of bdellopasts with deformations toward the predator inside | 129 | 63.9 | - | - | 176 | 76.9 | - | - |
| Predation related sub-cellular features in HADA-bright prey cells investigated | | | | | | | | |
| # of HADA Rings (from outside or half-entered) | 51 | 25.2 | 235.84 | 28.40 | 17 | 7.4 | 243.43 | 38.54 |
| # of HADA Discs (from outside) | 28 | 13.9 | 213.42 | 31.81 | 20 | 8.7 | 188.50 | 47.52 |
| # of HADA Disc Seals (from inside) | 39 | 19.3 | 176.87 | 33.64 | 57 | 24.9 | 158.51 | 35.56 |
| # of HADA Ring Seals (from inside) | 7 | 3.5 | 228.57 | 55.98 | 7 | 3.1 | 234.00 | 33.72 |
| Predation related miscellaneous features in HADA-bright prey cells investigated | | | | | | | | |
| # of predator inside, but no clear discs/seal/ring | 78 | 38.6 | - | - | 107 | 46.7 | - | - |
| # discs/rings on prey OR bdelloplasts without any clearly labelled predator | 17 | 8.4 | - | - | 21 | 9.2 | - | - |

**Supplementary Table 2-** Systematic analysis of 3D reconstructed cells from 3D-SIM (see **Figure 2, Supplementary Movie** and **Supplementary Figure 2** for examples of these). HADA Rings are defined as clearly resolved rings of HADA modification on the prey PG proximal to the point of contact with the predator on the outside or inside of the prey. HADA Discs are defined as regions of HADA at the point of predator prey contact that were not resolved into rings, likely due to early contact by the predator. Seals are defined as patches of HADA at the point of contact with an internalised predator, likely indicative of the re-sealing of the hole in the prey PG. These Seals were in the form of either ‘Disc Seals’; filled discs of HADA (see **Supplementary Figure 2e- yellow arrowheads**) or ‘Ring Seals‘; rings of HADA of slightly smaller diameter than the initial entry pore (see **Supplementary Figure 2e- red arrowheads**).

| | Instances | % of instances | Average long axis diameter (nm) | Std-dev | Instances | % of instances | Average long axis diameter (nm) | Std-dev |
|---|---|---|---|---|---|---|---|---|
| | 15 minutes | | | | 30 minutes | | | |
| Number of interacting cells investigated | 45 | | | | 63 | | | |
| # of HADA RINGS | 37 | 82.2 | 205.24 | 35.29 | 56 | 88.8 | 210.98 | 54.86 |
| # of co-incident HADA RING-TADA Pore | 17 | 37.8 | 145.23 | 42.19 | 43 | 68.3 | 179.35 | 40.34 |
| # of HADA Discs | | | | | 7 | 11.1 | 254.27 | 55.07 |
| # of co-incident HADA Disc-TADA Pore | | | | | 4 | 6.3 | 243.0 | 40.75 |
| # of HADA patches | 8 | 17.8 | 231.63 | 52.20 | 2 | 3.2 | 259 | 43.84 |

**Supplementary Table 3-** Systematic analysis of 3D reconstructed cells from 3D-SIM (See **Figure 3**) with *E. coli imp4213*$^{-}$ permeable mutant strain. HADA Rings were clearly resolved rings of HADA modification on the prey PG proximal to the point of contact with the predator on the outside or the inside of the prey. In these experiments using this more permeable strain of prey, pores in the TADA were visible co-incident with the HADA Rings. Patches were regions of HADA at the point of predator prey contact that were not resolved into rings (Likely early contact by the predator at 15 minutes or nearly complete Disc at 30 minutes). Discs were patches of HADA at the point of contact with an internalised predator, likely the re-sealing of the hole in the prey PG and with this prey strain were seen co-incident with the patch of HADA.

## Supplementary Reference

1 Lambert, C. *et al.* Ankyrin-mediated self-protection during cell invasion by the bacterial predator *Bdellovibrio bacteriovorus*. *Nature communications* **6**, 8884, doi:10.1038/ncomms9884 (2015).